Aspects of Molecular Medicine 4 (2024) 100055

Contents lists available at ScienceDirect

Aspects of Molecular Medicine

journal homepage: www.journals.elsevier.com/aspects-of-molecular-medicine

BCL-2 and BAX expression and germ cell apoptosis following the intervention of 1-isothiocyanato-4-methylsulfinylbutane in cisplatin-induced testicular toxicity and sperm DNA fragmentation in Sprague-Dawley rat

Sunday Aderemi Adelakun [a,b,*], Olalekan Wasiu Akintunde [b], Babatunde Ogunlade [a], Akwu Bala Peter [c], Jacob Adewale Siyanbade [b]

[a] Department of Human Anatomy, Federal University of Technology, Akure, Nigeria
[b] Department of Anatomy, Ladoke Akintola University of Technology, Ogbomoso, Nigeria
[c] Department of Anatomy, Kogi State University, Anyigba, Nigeria

ARTICLE INFO

Handling Editor: Prof A Angelo Azzi

Keywords:
Isothiocyanates-4-methylsulfonyl butane
Cisplatin
Apoptosis
Testosterone
DNA fragmentation
Infertility
Male rats

ABSTRACT

Cisplatin (CP) has been used in clinical oncology but causes spermatogenesis damage. Isothiocyanato-4-methylsulfonylbutane (SFN) is a potent dietary bioactive agent that has been extensively studied for its effects on disease prevention. This study focused on the intervention of SFN on Germ cell apoptosis in CP-induced testicular toxicity and sperm DNA fragmentation (SDF). A total of ninety (90) male and ninety (90) female rats (weighing, 150–200 g, 12–14 weeks old) were assigned randomly into nine groups of ten (n = 10) rats each. Group A received normal saline, group B received a single dose of 10 mg/kg CP (i.p.), group C received 50 mg/kg bwt of SFN, group D received 100 mg/kg bwt of SFN, group E received 10 mg/kg bwt CP and 50 mg/kg bwt of SFN, group F received 10 mg/kg bwt CP and 100 mg/kg bwt of SFN, group G received 10 mg/kg bwt CP and 50 mg/kg bwt vitamin C, group H received 50 mg/kg bwt of SFN and 10 mg/kg bwt CP, Group I received 100 mg/kg bwt of SFN and 10 mg/kg bwt CP. The procedure lasted for 56 days. At the end of each treatment, the 90 male rats were introduced to the 90 female rats on the proestrus at a ratio of 1:1 for fertility tests. Testicular histopathological, apoptotic marker, immunoreactivity, sperm parameters, and SDF were investigated.

Cisplatin significantly decreases chromatin condensation/de-condensation levels, haploid germ cells, the number of fetuses, and BCL-2 expression. Also, CP increases SDF and BAX expression relative to control. Treatment with SFN increased BCL-2 expression, haploid germ cells, protected sperm chromatin condensation, improved microarchitecture of testes, and decreased SDF and BAX expression.

Therefore, SFN protects against CP-induced apoptosis by controlling BCL-2 and BAX expression and ameliorates SDF.

1. Introduction

Cisplatin (CP) has been used worldwide to treat various solid neoplasms, including lung, head, and neck colorectal, hematologic, and ovarian cancers (Ranasinghe et al., 2022). Cisplatin is one of the most commonly used cytotoxic anticancer medications due to its extensive usefulness in treating various tumors (Tchounwou et al., 2021). Cisplatin binds to the DNA of rapidly growing cells, resulting in anticancer activity and germ cell losses (Sayyed et al., 2021). Cisplatin may also affect spermatogenesis through inhibition of nucleic acid synthesis of germ cells and testosterone production by damage of Leydig cells and the effects of CP treatment on testicular function have been noted in human and other animal models (Hong et al., 2021). Animals administered CP develop severe testicular damage characterized by germ cell apoptosis, Leydig cell dysfunction, and testicular steroidogenic disorder leading to infertility (Ismail et al., 2023a,b). Cisplatin forms covalent adducts with the cellular DNA molecules terminates vital processes like replication and transcription and induces apoptosis which causes reproductive toxicity (Makled and Said, 2021). The main functions of testes are to produce spermatozoa and steroid hormones (Bhardwaj and

* Corresponding author. Department of Human Anatomy, Federal University of Technology, Akure, Nigeria
E-mail addresses: adelakunsa@futa.edu.ng, anasony2008@gmail.com (S.A. Adelakun).

https://doi.org/10.1016/j.amolm.2024.100055
Received 20 April 2024; Received in revised form 11 October 2024; Accepted 13 October 2024
Available online 16 October 2024

Panchal, 2021). The physical barrier, called the blood-testis-barrier (BTB), formed by adjacent Sertoli cells, restricts the passage of unwanted toxicants to the ad luminal part of the seminiferous tubules, and ensures a proper environment for spermatogenesis (Liu et al., 2021). Functional or structural disruption on BTB or Sertoli cells will lead to sub/infertility in males (Yan et al., 2024). Testicular toxicity accounts for about 50% of infertility cases in men (Selvaraju et al., 2021). The critical factors responsible for testicular toxicity include hormonal, environmental, behavioral, and nutritional imbalances (Li and Spade, 2021). Therapeutic drugs (Cisplatin) can often adversely affect male fertility by injuring testicular germ cells or disturbing hormonal levels leading to decreased semen quality (Rahimi et al., 2022).

Vitamin C, also known as Ascorbic acid, is the most potent antioxidant that may shield biological systems from oxidative damage and is the first line of defense against many oxidizing environments (Yadegari et al., 2024). It can capture free radicals in the aqueous phase before they reach lipids because of its water solubility (Hamed et al., 2023). It is numerous dioxygenase enzymes, which are involved in the production of collagen and neurotransmitters like dopamine, norepinephrine, and serotonin, require ascorbic acid as a cofactor (Zylinska et al., 2023). Additionally, it can block LDL, which prevents cell death by reducing the peroxidation of membrane phospholipids (Wu et al., 2024). In the testis, vitamin C is regarded as a primary antioxidant because it inhibits sperm agglutination and neutralizes reactive oxygen species (ROS). It replenishes vitamin E, stops lipid peroxidation, donates electrons to redox systems, and guards against hydrogen peroxide radical-induced DNA damage (Moreira et al., 2022).

1-isothiocyanato-4-methylsulfinyl butane (SFN) is the most active natural product found in crucifers such as broccoli sprouts, cabbage, and kale with the potential of lowering the risk of cancer, oxidative stress-induced tissue injury, and age-related diseases, its chemopreventive qualities have drawn a lot of interest in recent years (Adelakun et al., 2023a; Bozic et al., 2022; Kalpana et al., 2013). 1-isothiocyanato-4-methylsulfinyl butane exists as a component of commonly consumed vegetables and it is especially abundant in broccoli (Ogunlade et al., 2020). 1-isothiocyanato-4-methylsulfinyl butane possesses anti-proliferative activities and can effectively halt the initiation and progression of chemically induced tissue damage in animals (Olayanju et al., 2024). Also, SFN emerges as a biologically active product resulting from the hydrolysis of glucosinolates, secondary metabolites found in plants from the Brassicaceae family (Kaiser et al., 2021). The conversion of glucosinolates into bioactive forms occurs through the process of hydrolysis, catalyzed either by the endogenous enzyme myrosinase (β-thioglucosidase) or human gastrointestinal microbiota (Kamal et al., 2022). Like other isothiocyanates, SFN has shown a wide range of positive health effects, including anti-inflammatory and antioxidant, tumor cell growth suppression, antidiabetic, cardioprotective, and other positive health effects (Rafiei et al., 2020). Unique structures, physical characteristics, and pharmacological potentials distinguish the several isothiocyanate precursors found in nature, including glucosinolates like glucoraphanin and gluconastrin (Coscueta et al., 2022). The key pharmacophore that determines the bioactivity of the SFN molecule is its isothiocyanate functional group (Kamal et al., 2020). 1-isothiocyanato-4-methylsulfinyl butane has garnered increased popularity in recent years, primarily due to its recognized anticancer potential (Mangla et al., 2021). Research reports suggest that SFN induces apoptosis in tumor cells through both intrinsic and extrinsic apoptotic pathways (Nandini et al., 2020). 1-isothiocyanato-4-methylsulfinyl butane also activates the antioxidant defense system by regulating nuclear factor erythroid 2-related factor 2 (Nrf2)/Kelch-like ECH-associated protein 1(Keap1)-ARE Kelch-like ECH-associating protein 1-antioxidant response element signaling, which is involved in a wide range of protective functions, such as antioxidant, anti-inflammatory, anticancer, and anti-apoptotic effects (Mahn et al., 2022). These properties have suggested the potential use of SFN as a therapeutic agent. Therefore, the aim of this study focused on BCL-2 and BAX expression and Germ cell apoptosis following the intervention of 1-isothiocyanato-4-methylsulfonylbutane in cisplatin-induced testicular toxicity and sperm DNA fragmentation in Sprague-Dawley rat.

2. Materials and methods

2.1. Chemicals, drugs, and reagents

The anticancer drug, cisplatin (50 mg/50 ml: Celplat TM 50), and vitamin C were obtained from the pharmacy Department of LAUTECH Teaching Hospital, Ogbomoso. 1-isothiocyanato-4-methylsulfonyl butane (SFN) was procured from Smoky Mountain Naturals, LLC, Lexington, USA. The ELISA kits for hormone profiles were obtained from Randox Laboratories Ltd., Admore Diamond Road, Crumlin, Co., Antrim, United Kingdom. Other histological staining reagents were sought. All other reagents that were used were of analytical grades.

2.2. Preparation of 1-isothiocyanato-4-methylsulfinylbutane

1-Isothiocyanato-4-methylsulfonylbutane was obtained from Sigma-Aldrich, USA. Two grams of 1-Isothiocyanato-4-methyl-sulfinylbutane were dissolved in 400 ml normal saline at 50 mg/kg and 100 mg/kg body weight concentration of 1% solution.

2.3. Preparation of vitamin C

Vitamin C (ascorbic acid) solution was prepared by dissolving five hundred milligrams (500 mg) of vitamin C in 100 ml of 0.9% w/v normal saline solution at a concentration of 50 mg/kg body weight.

2.4. Population, source, and maintenance of experimental animals

In the Faculty of Basic Medical Sciences, Ladoke Akintola University of Technology, Ogbomoso, Nigeria, Experimental Animal House, 90 sexually mature male and 90 female Sprague-Dawley rats were raised. The 90 female rats were used only for fertility tests and were not treated in the same way as male rats. The animals were housed in cages and given two weeks to acclimate before the experiment began. The rats were kept in a regular natural photoperiodic cycle of 12 h of darkness and 12 h of light (D: L; 12:12h dark/light cycle) at room temperature (25–32 °C) and humidity of 50–55%. Every day, their cages were cleaned. The animals were given conventional rat chow at a daily dose of 100 g/kg, as suggested by the International Centre for Diarrheal Disease Research in Bangladesh (ICDDR, B). Water is available ad libitum. The rats' body weight was recorded using an electronic analytical and precision balance (Mettler Toledo; Microstep (Pty) Ltd., Greifensee, Switzerland) at procurement, throughout the acclimatization period, at the start of administrations, and once a week throughout administration. All experimental studies were performed in conformity to the "Guide to the Resources for the Treatment and Use of Laboratory Animals". National Research Council, Department of Health and Human Services (National Institute of Health NIH, 1985) and in compliance with the recommendation of the Health Research Ethical Committee of the College of Health Sciences, the Ladoke Akintola University of Technology, Ogbomoso, Nigeria with registration number (LAUTECH/CHS/REC/02/003).

2.5. Experimental design

A total of ninety (90) male and ninety (90) female healthy adult Sprague-Dawley rats (weighing, 150–200 g, 12–14 weeks old) were utilized in this research. The 90 female rats were used only for fertility tests and were not treated in the same way as male rats. The 90 male rats were randomly assigned into nine groups (A, B, C, D, E, F, G, H, and I) of ten (n = 10) rats each. Group A: Animals in group A served as control and each was given 2 ml of normal saline daily. Group B: On the first

day, each of the rats in group B was given a single dose of 10 mg/kg cisplatin (i.p.). Group C: Each of the rats in group C was given 50 mg/kg body weight of 1-isothiocyanato-4-methylsulfinylbutane once daily. D: Each of the rats in group D was given 100 mg/kg body weight of 1-isothiocyanato-4-methylsulfinylbutane once daily. Group E: Each of the rats in group E was given a single dose of 10 mg/kg cisplatin (i.p.) on the 1st day followed by 50 mg/kg body weight of 1-isothiocyanato-4-methylsulfinylbutane once daily). Group F: Each of the rats in group F was given a single dose of 10 mg/kg cisplatin (i.p.) on the 1st day followed by 100 mg/kg body weight of 1-isothiocyanato-4-methylsulfinylbutane once daily). Group G: Each of the rats in group G was given a single dose of 10 mg/kg cisplatin on the first day followed by 50 mg/kg vitamin C as a standard drug once daily. Group H: Each of the rats in group H was given 50 mg/kg body weight of 1-isothiocyanato-4-methylsulfinylbutane once daily followed by a single dose of 10 mg/kg cisplatin (i.p.) on the last day. Group I: Each of the rats in group I was given 100 mg/kg body weight of 1-isothiocyanato-4-methylsulfinylbutane once daily followed by a single dose of 10 mg/kg cisplatin (i.p.) on the last day. The procedure lasted for 56 days. At the end of each treatment, the 90 male rats were introduced to 90 female rats on the proestrus day of their cycle at a ratio of 1:1 for the fertility test. The concentration of the SNF, Cisplatin, and Vit.C was determined through a pilot study [Table 1].

2.6. Determination of cyclicity

Every animal's estrous cycle was documented for two weeks using vaginal lavage collected between eight and nine in the morning the day before the experiment started. By amending the procedure outlined by Adelakun et al. (2022a), and Ucheya and Biose (2010), cyclicity was ascertained. In a nutshell, a new plastic Pasteur pipette filled with fresh normal saline was introduced into the vaginal canal at a depth of 1 mm and irrigated. After that, the lavage was spread out on a tiny slide and examined under a microscope until it dried. The proestrus day of the cycle was identified by the presence of big nucleated cells on the slide together with a few leucocytes.

A marked male rat from a known group of males was matched 1:1 to a marked female cage on the proestrus day of each rat's cycle. Overnight, these paired animals remained together. On the morning of the cycle's estrous day, after pairing, between 8:00 and 9:00 a.m., vaginal lavage was performed. Day 1 of pregnancy was determined by the presence of spermatozoa in the lavage (Ratnasooriya and Dharmasiri, 2000; Adelakun et al., 2024a).

Table 1
Number of animals per group and dosage of treatment rendered.

Animals grouping	Number of male rats	Animal Induction and treatment
Group A	10	10 ml of 0.9% normal saline per kg bwt orally for 56 days
Group B	10	10 mg/kg cisplatin (i.p.) only on the 1st day
Group C	10	50 mg/kg bwt SFN only orally for 56 days
Group D	10	100 mg/kg bwt SFN only orally for 56 days
Group E	10	10 mg/kg cisplatin (i.p.) on the 1st day + 50 mg/kg bwt SFN orally for 56 days
Grouop F	10	10 mg/kg cisplatin (i.p.) on the 1st day + 100 mg/kg bwt SFN orally for 56 days
Group G	10	10 mg/kg cisplatin (i.p.) on the 1st day + 50 mg/kg vitamin C orally for 56 days
Group H	10	50 mg/kg bwt SFN orally for 56 days + 10 mg/kg cisplatin (i.p.) on the last day
Group I	10	100 mg/kg bwt SFN orally for 56 days + 10 mg/kg cisplatin (i.p.) on the last day
Fertility test	Fertility test: ratio 1:1 (1 male rat: 1 female rat)	

SFN: 1-isothiocyanato-4-methyl sulfonyl butane, CP: Cisplatin, i.p: Intraperitoneally, total number of male rats = 90, total number of female rats = 90, number of rat per group = 10. The procedure lasted for 56 days (Duration of spermatogenesis in rat being 51.6–56 days (Sasso-Cerri, 2009).

2.7. Collection of fetuses

On the 20th day of gestation, fetuses were removed from pregnant rats by ventral laparotomy and examined. The number of live fetuses was recorded. Live fetuses were removed from the uterus, weighed, and examined for gross malformations. The crown-rump length was also measured using methods described by Oderinde et al. (2002).

2.8. Animal sacrifice and sample collection

Before collecting blood from the retro-orbital venous plexus into simple tubes, the final weights of each rat were obtained. On day 56, the rats were euthanized with thiopental (100 mg/kg, i.p.) (Adelakun et al., 2022b) and sacrificed by cervical dislocation. Serum samples were collected by centrifuging the blood at 3000g for 10 min. Each animal's testis weight was measured using an electronic analytical and precision balance (Mettler Toledo; Microstep (Pty) Ltd., Greifensee, Switzerland). The testes volumes were determined using the water displacement technique. The average value obtained for each parameter was treated as one observation, and results were reported as g/100 g body weight (Adelakun et al., 2021a). Each animal's testis and pituitary gland were fixed in Bouin's fluid and 10% formol-saline respectively for histological and morphometric examination. Each animal's serum and leftover testes were preserved at −20 °C for further biochemical testing (Adelakun et al., 2017, 2018; Ogunlade et al., 2021).

2.9. Testicular homogenate preparation

The testes were carefully removed from the rats, washed, and homogenized with an ice-cold 1:5 w/v solution containing 0.25 M sucrose. To acquire post-mitochondrial fractions, centrifugation of the homogenates was performed at 3000 g for 10 min at 4 °C, and the resultant supernatant was kept at −20 °C to guarantee the maximal release of the testicular fractions (Adelakun et al., 2021b).

2.10. Epididymal sperm morphology

A normal sperm has an oval-shaped head, an intact midpiece, and an uncoiled single tail (Fig. 1). Abnormal sperm have head or tail defects, such as a large or misshapen head or a crooked or double tail (Fig. 1). For sperm abnormalities, smears were fixed with alcohol, stained with eosin Y, and then examined for morphological abnormalities. The morphological abnormalities were divided into head and tail defects. Sperm abnormalities of the mid-piece were included as part of the assessment of the sperm tail. The percentages of normal and abnormal-shaped sperms were calculated. The percentages of abnormal sperm in three fields were calculated according to a previous protocol (Aydogan and Barlas, 2006; Adelakun et al., 2020; Adelakun et al., 2021c)

2.11. Germ cell preparation

The testicular tissue preparation for flow cytometry was performed as described (Dey et al., 2000).

Briefly, the testicular tissue was obtained immediately after dissecting rats from the same region of the testis. To optimize the release of germ cells from the seminiferous tubule minces, the testicular tissue was promptly and finely minced in PBS, gently pushed through the syringe's hub, and then vortexed for a brief period. A nylon filter was then used to filter the cell suspension, and a drop of the filtrate was observed under the microscope to check the number and integrity of the released germ cells before fixing them in 80% chilled ethanol and storing them at 4 °C until flow cytometric analysis.

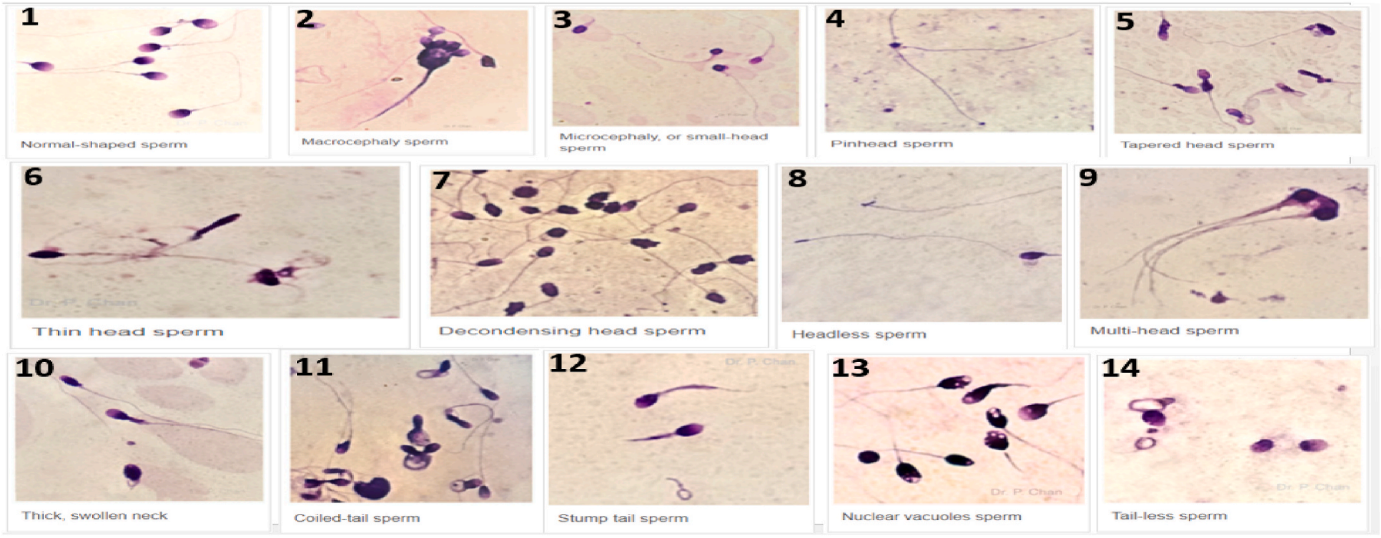

Fig. 1. Photomicrograph of normal and abnormal sperm morphology 1: Normal shaped sperm, 2: Macrocephaly sperm, 3: Microcephaly or small head sperm, 4: Pinhead sperm, 5: Tapered head sperm, 6: Thin head sperm, 7: Decondensing head sperm, 8: Headless sperm, 9: Multi-head sperm, 10: Tick swollen neck sperm, 11: Coiled-tail sperm, 12: Stump tail sperm, 13: Nuclear vacuoles sperm, 14: Tail-less sperm (Loma Linda University Center for Fertility & IVF © 2015–2024).

2.12. Flow cytometric determination of epididymal sperm ploidy and condensation/de-condensation

Before fixation, the epidydimal sperm samples underwent two PBS washes and were diluted. The samples were preserved at 4 °C until staining and were promptly fixed with 1 mL of ice-cold pure alcohol, dropped by drop with gentle shaking. Propidium iodide (PI) staining for DNA ploidy was done by Vindelov's (1977) protocol. Another sample was subjected to sodium dodecyl sulfate treatment and processed by the protocol outlined by Hacker-Klom et al. (1999) to measure the de-condensation. Flow cytometric analysis was aimed at measuring the parameters, such as (a) mature haploid spermatozoa percentage at 1 mL peak, (b) haploid round spermatids percentage at 1 mL peak, and (c) diploid spermatozoa percentage at 2 mL peak. Chromatin condensation percentage and chromatin de condensation percentage were analyzed using FACSCalibur™ flow cytometer (Becton Dickinson, Sunnyvale, California, USA)

2.13. Flow cytometric analysis of apoptosis with annexin V–fluorescein isothiocyanate/PI

For the annexin V assay, testicular cells were stained with fluorescein isothiocyanate (FITC)-conjugated annexin V using the ApoAlert kit from Clontech (Palo Alto, California, USA) according to the manufacturer's instructions. Testicular cell samples were fixed in 100 mL of cold 1% paraformaldehyde in PBS for 1 h at 4 °C on a 96-well plate for this investigation. The cells were shaken on a shaker during the fixation procedure and pipetted many times while paraformaldehyde was added to avoid cell clumping. The fixed cells underwent two washes in 200 mL of PBS after a 5-minute centrifugation. After being suspended in 200 mL of PBS containing 50 mg/mL of ribonuclease A (RNase A) and 50 mg/mL of PI, the cells were incubated at 37 °C for 30 min. The flow cytometric analyses were performed on a FACS Calibur cytometer using CellQuest Pro software (Becton Dickinson) for data acquisition and analysis (Juan et al., 2012).

2.14. Determination of sperm DNA fragmentation

An alkaline single-cell gel electrophoresis (comet) experiment was used to measure sperm DNA fragmentation (Hughes et al., 1997; Donnelly et al., 1999). To create the epididymal fluid ratio of 1:20, 0.1 ml of fluid was mixed with 1.9 ml of PureSperm® wash (Nidacon International AB, Mölndal, Sweden). Aliquots of neat epididymal sperm were adjusted to a sperm concentration of 6 x 10^6/ml using a Neubauer-improved hemocytometer. To avoid induced DNA damage, all remaining processes were performed in a climate-controlled environment (20 °C) with yellow light. This was accomplished by adjustments to the procedures employed by Agbaje et al. (2007).

Frosted microscope slides were gently heated before being coated with 100 l of 0.5% normal melting point agarose in phosphate-buffered saline and immediately covered with a glass coverslip (22 mm 50 mm). To allow the agarose to harden, the slides were kept at room temperature (18 °C). The coverslips were removed, and 75 l of 0.5% low melting point agarose was combined with 10 l of diluted epididymal sperm ($6X10^6$/ml). This cell solution was pipetted over the first layer of gel, which was then covered with a glass coverslip and allowed to harden at room temperature.

The coverslips were removed, and the slides were submerged for 1 h at 4 °C in a Coplin jar containing 22.5 ml of new lysis solution (2.5 M NaCl, 100 mM EDTA, and 10 mM Tris (pH 10), with 1% Triton X 100 added right before use). Following that, 2.5 mL of 0.1 M dithiothreitol was added for 30 min at 4 °C to obtain a final concentration of 10 mM. After that, 2.5 mL of 40 mM lithium diiodosalicylate was added to obtain a final concentration of 4 mM, which was then incubated at room temperature for 90 min. The slides were taken out of the lysis solution and drained of any remaining fluid.

To allow the exposed DNA to unwind, a fresh alkaline buffer (300 mM NaOH/1 mM EDTA) was produced and placed into a horizontal gel electrophoresis tank at 24V/300 mA for 30 min. The slides were taken from the tank, drained, and flooded three times with neutralization buffer (0.4 M Tris; pH 7.5), to eliminate any leftover alkali or detergents that may interfere with staining. PicoGreen dye was used to stain the slides, which were then covered with a glass coverslip and kept in a humidified container in the dark at 4 °C overnight. Images of comets were acquired on three slides for each group using a Leica DM fluorescence microscope and CCD camera. CometscoreTM software (TriTek Corp., Sumerduck, VA) was used to examine the images.

2.15. TUNEL assay

As directed by the manufacturer, a TUNEL Kit (Roche in situ cell death detection kit, Fluorescein) was used to assess apoptosis in spermatogenesis cells in the testicular tissue slices. The deoxynucleotidyl transferase marker, which identifies the free 3.-OH in the final regions of

nucleic acids, and the terminal enzyme's detection of DNA breakage serve as the foundation for the TUNEL test diagnosis. TUNEL can distinguish between two types of cells: non-apoptotic cells with intact DNA and apoptotic cells with damaged DNA (positive-TUNEL and negative-TUNEL, respectively).

2.16. Histopathological and spermatogenesis index assay

Melted paraffin was applied to the samples to block them after they underwent the tissue processing procedures. An apparatus called a microtome set was used to cut paraffin blocks into 5-μm pieces and the samples were stained with hematoxylin and eosin (Mehranjani and Taefi, 2012; Adelakun et al., 2023b; Adelakun et al., 2024b; Ukwenya et al., 2020). Each testis's 100 seminiferous tubules were also analyzed for this purpose to assess the following index: The tubule differentiation index, or TDI, is the percentage of seminiferous tubules—those with three layers or more of germinal cells derived from type a spermatogonia cells—that possessed this index in the testicular tissue of each rat was computed. Spermatogenic Index (SPI): This index indicates the percentage of seminiferous tubules with normal spermatogenesis and containing sperm (Rezvanfar et al., 2008; Olawuyi et al., 2019). Sertoli Cell Index (SCI): This index was compared to the germinal cells number by the Sertoli cells number (spermatogonia þ spermatocyte/Sertoli cells per each seminiferous tube (Malmir et al., 2018), Meiosis Index (MI): For meiosis Index, the ratio of the round spermatozoa number to primary spermatocytes was calculated.

2.17. Immunohistochemical staining of testicular BCL-2, and BAX

Testicular BCL-2, and BAX immunohistochemistry: Fixed and paraffin-embedded testicular tissues were sectioned at 4 m for immunohistochemistry. Immunohistochemical experiments were carried out using the LSAB® HRP kit (Dako, Ltd), anti-mouse BCL-2 monoclonal antibody (Dako, Ltd), and monoclonal rabbit anti-BAX antibody (Dako, Ltd). In summary, after deparaffinization and rehydration of sections, antigen retrieval was conducted for 10 min using a warmed buffer solution of citrate (pH 6.0) and EDTA (pH 9.0), followed by protein block for 15 min using 3% Hydrogen peroxide. For 1 h, the slice was incubated with primary antibodies (anti-mouse, BCL-2, and BAX) in a humidified atmosphere at room temperature.

Sections were then incubated for 15 min at room temperature in the biotinylated link, followed by 15 min in streptavidin-HRP. For the chromogen reaction, the section was incubated in diaminobenzidine substrate solution for 5 min before being counterstained in Gill's hematoxylin for 10 s. Using a light microscope (X400), the tissue slides were immunostained for BCL-2 and BAX. Random microscopic fields were chosen. There were five fields per slide and seven slides per rat. Digital photomicrographs were imported into Image J software for quantification of BCL-2 and BAX immunoreactivity, and the proportion of positive (DAB) stained nuclear area was calculated using the ImmunoRatio plugin. The ImmunoRatio application computes the percentage of the positively stained nuclear area using a color deconvolution algorithm that separates the staining component (in this instance; the DAB chromogen and the hematoxylin counterstaining) and adaptive thresh holding for nuclear area segmentation (Atalay et al.,2012; Elham et al., 2016; Tuominen et al.,2010).

2.18. Statistical analysis

The data were presented as mean ± standard error of the mean (S.E.M.). The Instat-3 computer program (v2.04, GraphPad Software Inc., San Diego, CA, USA) was used to analyze the data and evaluate the significant differences; the comparison of means between each experimental group was made using one-way ANOVA with Newman-Keuls Multiple Comparison significant difference test. If $p < 0.05$, the difference was judged significant.

3. Results

3.1. Sperm parameters

The flow cytometry analysis of ploidy and condensation of epididymal sperm about the effect of SFN and CP are summarized in Table 2. The percentage of haploid sperm in the CP-treated group was significantly lower than that of the control. The percentage of diploid sperm and spermatids in rats treated with SFN present an insignificant lower value compared to the control rats. Moreover, the mean sperm chromatin condensation/de-condensation values were reduced significantly in the CP-treated rats compared with control groups. In contrast, when SFN was administered before and after CP exposure, SFN significantly ameliorated and protected the effects of CP on the percentages of ploidy levels in the sperm. This combined treatment showed significant protection of sperm chromatin condensation/de-condensation ratio compared with the CP-treated groups and appeared close to the control levels [Table 2].

The results of the sperm morphology show a significant ($p < 0.05$) decrease in normal sperm morphology and an increase in abnormal sperm morphology in rats treated with cisplatin (CP) alone when compared to the control group. However, pretreatment and post-treatment with SFN presented a significant ($p < 0.05$) decrease in abnormal sperm morphology and an increase in normal sperm morphology compared to CP alone exposed group [Table 2, Fig. 2].

3.2. Fertility test

There was observed lower fertility index in in CP and CP + Vit.C treated group compared to control and other experimental groups. Fertility index in control, SFN only, SFN + CP is higher than that of CP + SFN. There were no observable malformations on the fetuses of dams that were mated with male rats treated with CP and CP + Vit.C but there was no significant difference ($p > 0.05$) in fetuses' weight and crown-rump length however, administration of SFN alone and co administration of CP and SFN insignificantly increase the number of fetuses as compared with CP and CP + Vit.C administered groups ($p > 0.05$). Also, there was a significant decrease ($P < 0.05$) in the number of fetuses of dams mated with male rats injected with CP and CP + Vit.C treated rats compared to control. However, treatment, pretreatment, and post-treatment significantly increase the number of fetuses of dams mated with male rats SFN, CP + SFN, and SFN + CP treated groups in comparison with CP and CP + Vit.C treated groups [Table 3].

3.3. Testicular apoptotic

The number of apoptotic and necrotic cells showed a significant increase in response to cisplatin treatment compared with the control groups. Meanwhile, the viable cells in the testes significantly decreased after cisplatin treatment. Pretreatment and post-treatment with SFN protected germ cell viability, evidenced by a significant increase in the viable cells associated with a significant decrease in the apoptotic and necrotic cells compared with the CP-treated rats [Fig. 3].

3.4. Sperm DNA fragmentation

When compared to controls, cisplatin (CP) administration significantly increases tail length, tail moment, and tail %DNA ($p < 0.05$). However, there was a significant decrease in tail length, tail moment, and tail DNA percentage in the SFN group ($p < 0.05$) as compared to CP alone exposed rats. Also, the vitamin C (CP + Vit.C) post-treated group had a significantly increased tail length, tail moment, and tail DNA percentage ($p < 0.05$) when compared to the control. But, there was no significant difference between the CP and CP + Vit.C treated groups ($p > 0.05$). Administration of SFN alone substantially reduced tail length, tail moment, and tail DNA percentage when compared to the CP-alone

Table 2
Impact of 1-isothiocyanato-4-methyl sulfinyl butane (SFN) on sperm morphology, DNA ploidy levels, chromatin condensation, and de-condensation in cisplatin (CP) induced Alterations in Pituitary-Gonadal Axis.

Treatment groups	Sperm parameters						
	Normal morphology (%)	Abnormal morphology (%)	Haploid sperm	Diploid sperm	Spermatid	Condensation	De-condensation
A	80.67 ± 4.33	19.33 ± 4.33	83.25 ± 5.67	16.75 ± 5.67	2.37 ± 0.38	84.24 ± 5.88	118.40 ± 6.30
B	15.33 ± 2.91*	84.67 ± 2.91*	67.93 ± 4.10*	32.07 ± 4.10*	37.75 ± 8.96*	32.82 ± 4.23*	68.43 ± 4.79*
C	83.33 ± 5.21 $^{\alpha\beta}$	16.67 ± 5.21 $^{\alpha\beta}$	85.51 ± 4.59 $^{\alpha\beta}$	14.59 ± 4.61 $^{\alpha\beta}$	2.10 ± 0.33 $^{\alpha\beta}$	87.96 ± 5.78 $^{\alpha\beta}$	124.10 ± 6.37 $^{\alpha\beta}$
D	89.33 ± 3.84 $^{\alpha\beta}$	10.67 ± 3.84 $^{\alpha\beta}$	86.48 ± 4.63 $^{\alpha\beta}$	13.52 ± 4.63 $^{\alpha\beta}$	2.07 ± 0.31 $^{\alpha\beta}$	88.83 ± 4.68 $^{\alpha\beta}$	126.10 ± 7.18 $^{\alpha\beta}$
E	72.33 ± 4.33 $^{\alpha\beta}$	27.67 ± 4.33 $^{\alpha\beta}$	77.08 ± 4.66 $^{\alpha\beta}$	22.92 ± 4.66 $^{\alpha\beta}$	15.66 ± 2.93 $^{\alpha\beta}$	71.92 ± 6.09 $^{\alpha\beta}$	109.10 ± 6.99 $^{\alpha\beta}$
F	75.33 ± 3.76 $^{\alpha\beta}$	24.67 ± 3.76 $^{\alpha\beta}$	76.76 ± 5.55 $^{\alpha\beta}$	23.24 ± 5.55 $^{\alpha\beta}$	15.97 ± 3.30 $^{\alpha\beta}$	74.24 ± 7.02 $^{\alpha\beta}$	108.60 ± 7.88 $^{\alpha\beta}$
G	33.33 ± 4.41*	66.67 ± 4.41*	69.98 ± 4.23*	30.02 ± 4.23*	32.98 ± 9.21*	26.36 ± 3.20 *	62.63 ± 3.79*
H	76.33 ± 3.76 $^{\alpha\beta}$	23.67 ± 3.76 $^{\alpha\beta}$	80.84 ± 4.97 $^{\alpha\beta}$	19.16 ± 4.97 $^{\alpha\beta}$	13.07 ± 2.38 $^{\alpha\beta}$	73.02 ± 8.96 $^{\alpha\beta}$	116.50 ± 5.04 $^{\alpha\beta}$
I	79.67 ± 2.60 $^{\alpha\beta}$	20.33 ± 2.60 $^{\alpha\beta}$	81.75 ± 5.05 $^{\alpha\beta}$	18.25 ± 5.05 $^{\alpha\beta}$	12.87 ± 3.28 $^{\alpha\beta}$	74.20 ± 7.83 $^{\alpha\beta}$	117.00 ± 5.76 $^{\alpha\beta}$

Data expressed as Mean ± S.E.M, n = 10 in each group, *: represents a significant difference from control, α: represents a significant difference from CP, β: represents a significant difference from CP + Vit.C at ($p < 0.05$), One-Way ANOVA followed by Newman-Keuls multiple comparisons test.
A: Control, B: 10 mg/kg CP, C: 50 mg/kg SFN, D: 100 mg/kg SFN, E: 10 mg/kg CP+50 mg/kg SFN, F: 10 mg/kg CP + 100 mg/kg SFN, G: 10 mg/kg CP + Vit.C, H: 50 mg/kg SFN + 10 mg/kg CP, I: 100 mg/kg+ 10 mg/kg CP.

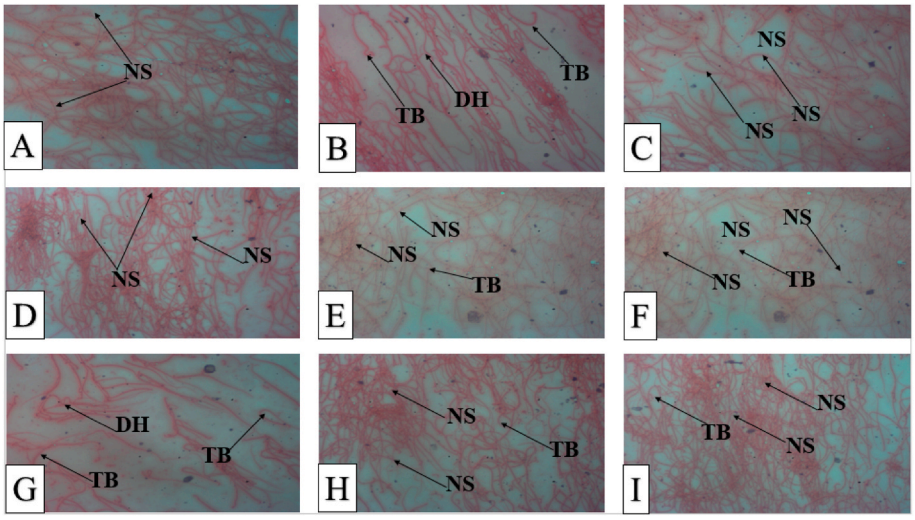

Fig. 2. Sperm Morphology (Head defects, midpiece defects, and tail defects) of A: Control, B: 10 mg/kg CP, C: 50 mg/kg SFN, D: 100 mg/kg SFN, E: 10 mg/kg CP+50 mg/kg SFN, F: 10 mg/kg CP + 100 mg/kg SFN, G: 10 mg/kg CP + Vit. C, H: 50 mg/kg SFN +10 mg/kg CP, I: 100 mg/kg+ 10 mg/kg CP. Showing DH: Detached, NS: Normal sperm, TB: Twisted body at MG: X400, Stain: Eosin.

treated group ($p < 0.05$) [Fig. 4A-C].

3.5. Positive-TUNEL spermatocyte, long spermatid, round spermatid, Sertoli and Leydig cells assay

Cisplatin (CP) exposure presents a significant increase in positive-TUNEL spermatocyte, long spermatid, round spermatid, Sertoli, and Leydig cells population compared to the control group ($p < 0.05$). However, Post-treatment and pretreatment with SFN significantly reduced positive-TUNEL congregation of spermatocyte, long spermatid, round spermatid, Sertoli, and Leydig cells as compared to CP alone exposed rats group ($p < 0.05$). There was no significant difference between CP alone injected rats and CP + Vit.C treated rats ($P > 0.05$). Administration of SFN alone substantially reduces positive TUNEL spermatocyte, long spermatid, round spermatid, Sertoli, and Leydig cell populations compared to CP alone treated rats [Fig. 5A-E].

3.6. Spermatogenesis index

The cisplatin-treated group showed a significant reduction in tubule differentiation, spermatogenic, and meiosis index compared to the control group. However, pretreatment and post-treatment with SFN significantly ($P < 0.05$) increased tubule differentiation, spermatogenic, and meiosis index compared to the group that received only CP and CP + Vit.C ($p < 0.05$). Also, CP alone exposed animals' exhibit a significant decrease in Sertoli cell index compared to the control group. However, post-treated and pretreated with SFN increased Sertolic cell index compared to CP alone exposed animals ($p < 0.05$). Groups treated with SFN present higher values in the Sertoli cell index than the CP + Vit.C treated group. Moreover, administration of SFN alone significantly increases ($p < 0.05$) spermatogenesis index compared to CP alone animals [Fig. 6A-C].

3.7. Testicular histopathology

Control: Sections of the testis of the control showed normal rounded to oval seminiferous tubules separated by narrow interstitial spaces. Each tubule was bounded by a basement membrane and flat peritubular myoid cells. The seminiferous tubules were lined by stratified epithelium composed of two populations of cells; the spermatogenic cells (germinal epithelium) and supporting Sertoli cells [Fig. 7A].

CP: Testicular sections from the cisplatin-exposed group revealed many histological changes as compared to the control group. The seminiferous tubules appeared irregular with disorganized germinal epithelium. Spermatogenic cells were lost focally, leaving vacant gaps and a discernible drop in their quantity. A few spermatogenic cells had

Table 3
Impact of 1-isothiocyanato-4-methyl sulfonyl butane (SFN) on fertility in cisplatin (CP) induced Alterations in Pituitary-Gonadal (PG) Axis and Sperm DNA Fragmentation.

Treatment groups	Fertility parameters				
	No. of pregnancies	Fertility index (FI) (%)	Fetal number	Fetal weight (g)	Crown-rump Length (cm)
A	10	100.00	8.00 ± 0.30	4.05 ± 0.41	4.28 ± 0.41
B	1	10.00	1.50 ± 1.00*	3.54 ± 0.44	3.51 ± 0.31
C	10	100.00	8.00 ± 0.26 $^{\alpha,\beta}$	4.15 ± 0.51	3.72 ± 0.52
D	10	100.00	7.40 ± 0.31 $^{\alpha,\beta}$	4.12 ± 0.49	3.94 ± 0.41
E	7	70.00	5.00 ± 1.13 $^{\alpha,\beta}$	4.30 ± 0.48	3.74 ± 0.41
F	9	80.00	6.10 ± 0.72 $^{\alpha,\beta}$	4.26 ± 0.46	3.74 ± 0.36
G	2	20.00	2.56 ± 1.28*	3.88 ± 0.31	3.47 ± 0.42
H	9	90.00	6.20 ± 1.07 $^{\alpha,\beta}$	4.21 ± 0.16	4.08 ± 0.43
I	9	90.00	6.00 ± 1.01 $^{\alpha,\beta}$	4.15 ± 0.49	4.20 ± 0.45

Data expressed as Mean ± S.E.M, n = 10 in each group, *: represents a significant difference from control, α: represents a significant difference from CP, β: represents a significant difference from CP + Vit.C at ($p < 0.05$), One-Way ANOVA followed by Newman-Keuls multiple comparisons test.
A: Control, B: 10 mg/kg CP, C: 50 mg/kg SFN, D: 100 mg/kg SFN, E: 10 mg/kg CP+50 mg/kg SFN, F: 10 mg/kg CP + 100 mg/kg SFN, G: 10 mg/kg CP + Vit.C, H: 50 mg/kg SFN + 10 mg/kg CP, I: 100 mg/kg+ 10 mg/kg CP.

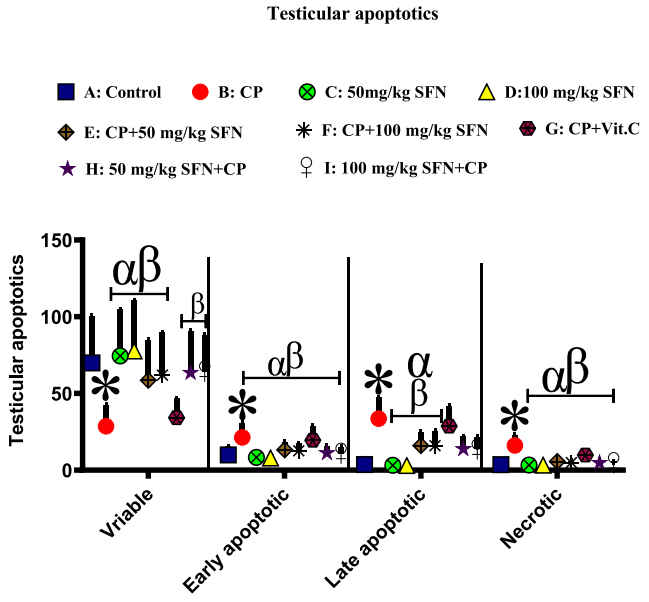

Fig. 3. Impact of 1-isothiocyanato-4-methylsulfinyl butane (SFN) on apoptotic in the testis in cisplatin (CP) induced Alterations in Pituitary-Gonadal (PG) Axis Data expressed as Mean ± S.E.M, n = 10 in each group, *: represents a significant difference from control, α: represents a significant difference from CP, β: represents a significant difference from CP + Vit.C. at ($p < 0.05$), One-Way ANOVA followed by Newman-Keuls multiple comparisons test.

pyknotic nuclei and looked shrunken. The lumina of tubules, which were packed with acidophilic hyaline streaks, was devoid of sperm. Certain tubules showed evidence of spermatogenic cells separating from the

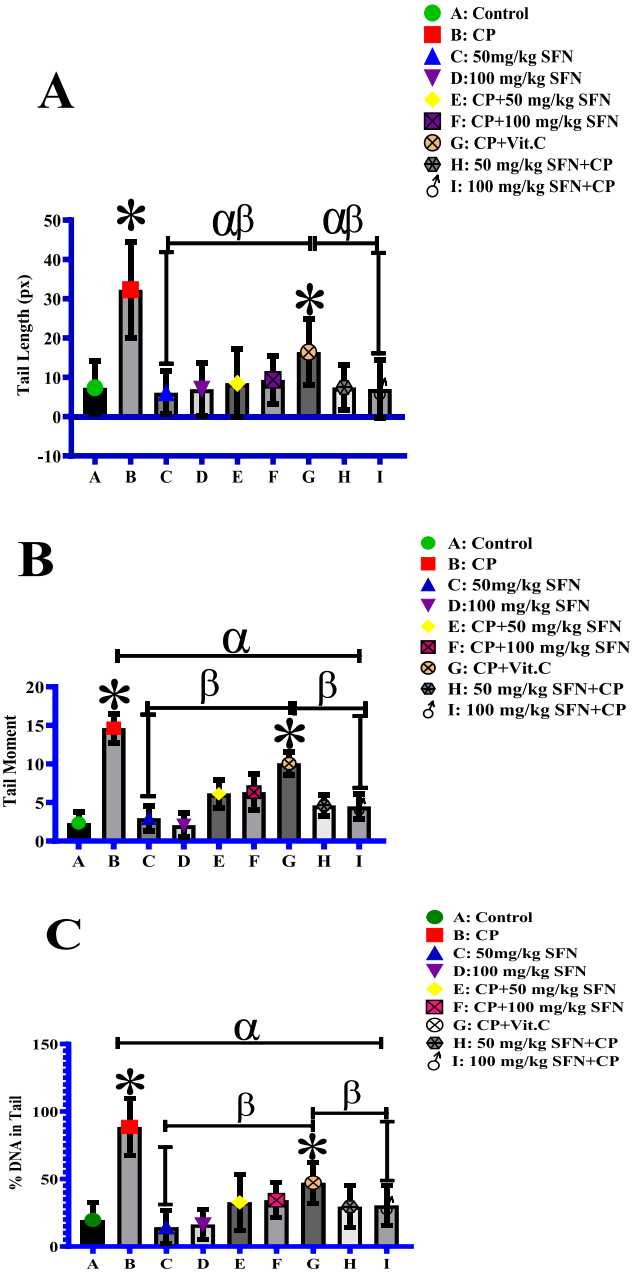

Fig. 4. Impact of 1-isothiocyanato-4-methyl sulfinylbutane (SFN) on sperm DNA fragmentation in cisplatin-induced sperm DNA fragmentations and pituitary-gonadal Axis toxicity in Sprague–Dawley rats. Data expressed as Mean ± S.E.M, n = 10 in each group, *: represents a significant difference from control, α: represents a significant difference from CP, β: represents a significant difference from CP + Vit.C at ($p < 0.05$), One-Way ANOVA followed by Newman-Keuls multiple comparisons test.

basal lamina. The interstitium was filled with many interstitial cells, congested blood arteries, and acidophilic hyaline material. It also seemed enlarged and vacuolated [Fig. 7B].

SFN (50 mg/kg and 100 mg/kg bwt): The section of the testis in this group shows normal spermatogenic cells. The spermatogenic cells represent different stages of spermatogenesis and are arranged in several layers. The basal layer was spermatogonia with rounded to oval nuclei. Primary spermatocytes were seen above the spermatogonia with large rounded nuclei. Numerous rows of spermatids were seen near the lumen of seminiferous tubules. In the tubule lumen, spermatozoa were visible. Periodically between cells that produce sperm on the basement

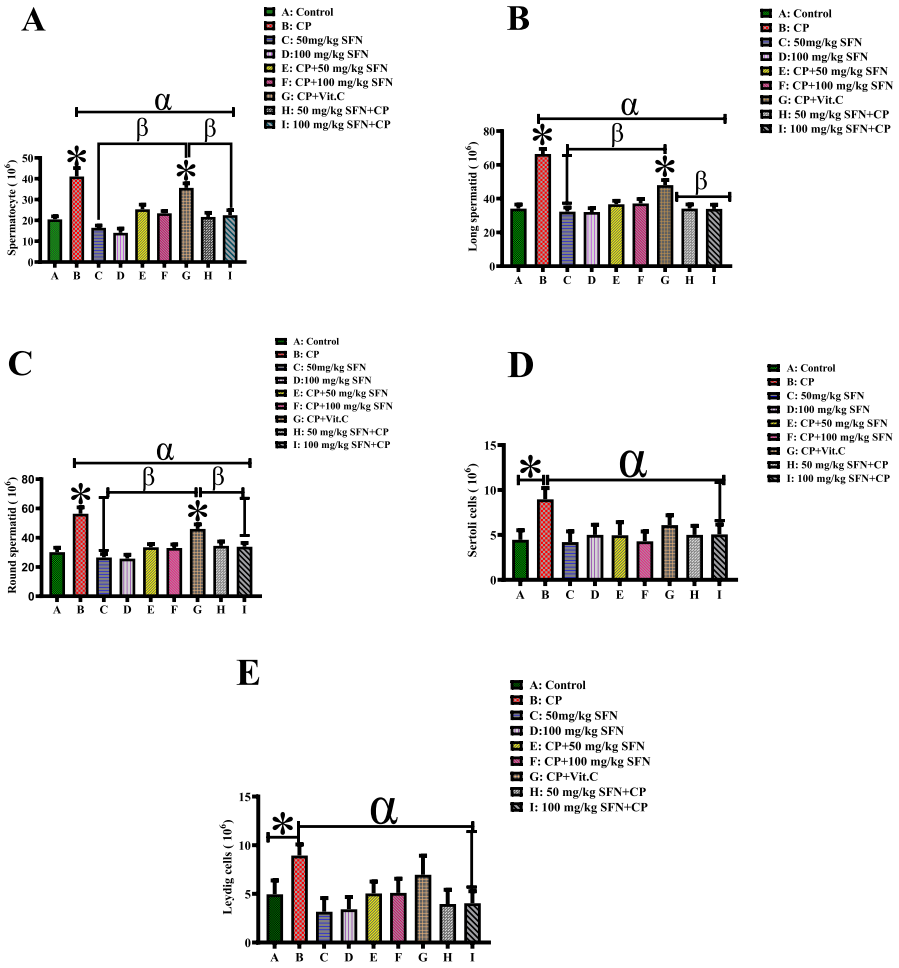

Fig. 5. Histogram showing the Impact of 1-isothiocyanato-4-methyl sulfonyl butane (SFN) on the TUNEL-positive spermatocyte, long spermatid, round spermatid, Sertoli and Leydig cell in cisplatin-induced sperm DNA fragmentations and pituitary-gonadal Axis toxicity in Sprague –Dawley rats. Data expressed as Mean ± S.E.M, n = 10 in each group, *: represents a significant difference from control, α: represents a significant difference from CP, β: represents a significant difference from CP + Vit.C at ($p < 0.05$), One-Way ANOVA followed by Newman-Keuls multiple comparisons test.

membrane, Sertoli cells were seen. Sertoli cells were elongated cells with basal, triangular, and vesicular nuclei. The narrow interstitial spaces in between tubules were occupied by loose connective tissues containing blood vessels and clusters of Leydig cells [7C & 7D].

CP + Vit.C: Sections from CP + Vit.C showed less degenerative alterations than the CP group. There were tubules containing mature spermatozoa in the lumen that showed normal structure. Other tubules, on the other hand, seemed to have deteriorated, with few germ cells and empty gaps. Somewhat expanded interstitial space [Fig. 7G].

CP + SFN and SFN + CP: Sections of the testis from the CP + SFN and SFN + CP group revealed a picture nearly similar to the control group with spermatogenic cells representing different stages of spermatogenesis and arranged in several layers. The basal layer was spermatogonia with rounded to oval nuclei. The lumen is filled with abundant sperm cells [Fig. 7E, F, 7H & 7I].

3.8. Immunohistochemical staining for testicular BAX

The localization of BAX (Fig. 8) proteins in the seminiferous tubules of boar testis was examined by immunohistochemical staining in the control and CP and SFN-treated groups. The expression of BAX protein was observed in spermatogonia, spermatocytes, and elongated spermatids. In the control group, Immunohistochemical examination of BAX expression revealed that the control groups' rats had only a few spermatozoa and spermatogonia with low BAX expression [Fig. 8A]. In cisplatin (CP) group had higher BAX expression levels in their seminiferous tubules in contrast to the control group [Fig. 8B]. The SFN (50 mg/kg bwt) treated group shows that BAX antibody labeling was low to moderate in every kind of germ cell [Fig. 7C]. Also, the SFN (100 mg/kg bwt) group revealed all types of germ cells and showed low to moderate BAX positivity [Fig. 8D]. Spermatogonia, spermatocytes, and elongated spermatids displayed modest BAX immunoreactivity in Group E: CP+50 mg/kg bwt [Fig. 8E]. And, the seminiferous tubules' sperm cells had a low level of BAX antibody in the CP+100 mg/kg bwt SFN treated group [Fig. 8F]. In the group treated with CP + Vit.C seminiferous tubules demonstrated enhanced BAX expression levels relative to the control group [Fig. 8G]. BAX immunoreactivity expression in germ cells was significantly reduced in the groups 50 mg/kg bwt + CP: and 100 mg/kg bwt + CP [Fig. 8H &I].

3.9. Testicular BAX immuno reactivity index

The testicular BAX immunoreactivity index increased significantly ($p < 0.05$) in the CP-alone treated group in comparison to the control group. But when compared with the CP alone treatment group, the animals pretreatment and post-treated with SFN demonstrate a significant reduction in the testicular BAX immunoreactivity index ($p < 0.05$). In addition, in comparison to the control group, the CP + Vit.C group had a

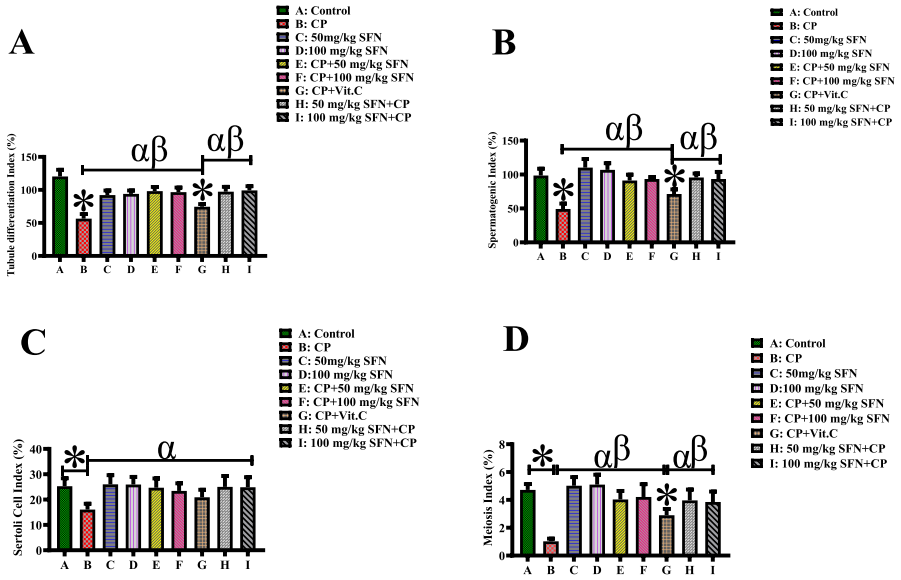

Fig. 6. Impact of 1-isothiocyanato-4-methyl sulfonyl butane (SFN) on Tubule Differentiation Index (TDI), Spermatogenic Index (SPI), Sertoli Cell Index (SCI), and Meiosis Index (MI) in cisplatin-induced sperm DNA fragmentations and pituitary-gonadal Axis toxicity in Sprague –Dawley rats. Data expressed as Mean ± S.E.M, n = 10 in each group, *: represents a significant difference from control, α: represents a significant difference from CP, β: represents a significant difference from CP + Vit.C at ($p < 0.05$), One-Way ANOVA followed by Newman-Keuls multiple comparisons test.

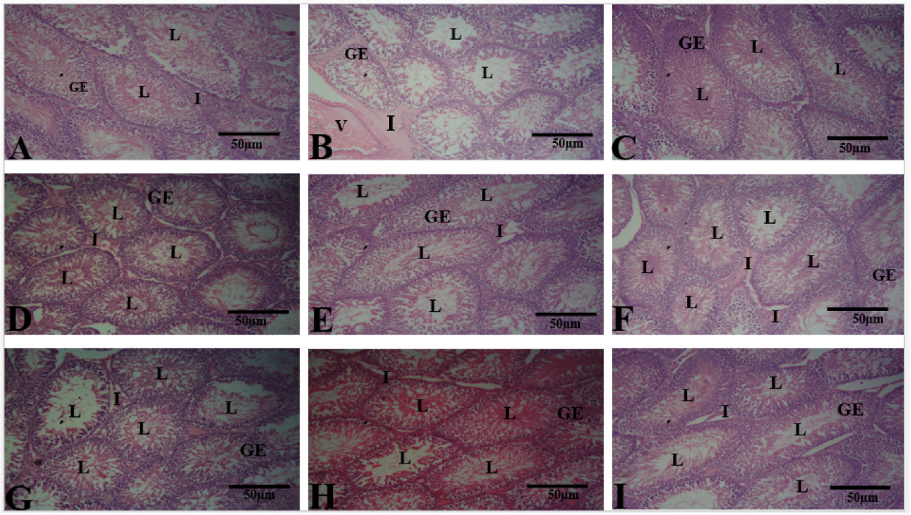

Fig. 7. Photomicrographs of testis after 8 weeks of administration, showing normal cellularity in the germinal epithelium (GE), lumen (L) filled with sperm cells, and interstitial cells of Leydig in the interstitium (I) in groups A (control), C (50 mg/kg bwt of SFN), D (100 mg/kg bwt of SFN) and E (CP+50 mg/kg bwt of SFN) and F (CP+100 mg/kg bwt SFN) and (50 mg/kg bwt of SFN + CP) and (100 mg/kg bwt of SFN + CP). Group B (10 mg/kg bwt of CP) demonstrates sloughed tissues, depleted germinal epithelium (GE), distorted seminiferous tubules, irregular seminiferous tubules with dead immotile multinucleated cells in the lumen, necrotic cells, empty lumen in some ST, vascular hemorrhage, disrupted basement membrane (blue arrow), and arrest of spermatogenesis. And group G (CP+50 mg/kg bwt of Vit. C) Revealed regenerating and irregular seminiferous tubules, [H & E, MagX100]. (For interpretation of the references to color in this figure legend, the reader is referred to the Web version of this article.)

substantial rise in the BAX immunoreactivity index in the testis ($p < 0.05$). However, there was no obvious disparity in the testis immunoreactivity index between the CP and CP + Vit.C therapy groups ($p > 0.05$) [Fig. 9].

3.10. Immunohistochemical staining for testicular BCL-2

Immunohistochemical investigation of BCL-2 expression in all germinal cells, including spermatogonia, spermatocytes, spermatids, and spermatozoa, revealed that control groups rats had high BCL-2 expression in all germinal cells, including spermatogonia, spermatocytes, spermatids, and spermatozoa [Fig. 10A]. The cisplatin (CP) group had lower BCL-2 expression levels in their seminiferous tubules [Fig. 10B]. In SFN alone treated group various types of germ cells showed high to moderate BCL-2 positivity [Fig. 10C and D]. BCL-2 immunoreactivity was seen in spermatogonia, spermatocytes, and elongated spermatids in SFN post-treated groups [Fig. 10E and F]. BCL-2 positivity was found to be high to moderate in numerous types of germ cells in CP + Vit. C group [Fig. 10G]. All kinds of germ cells, including spermatogonia, spermatocytes, spermatids, and spermatozoa, showed significant elevation of BCL-2 in SFN pretreated groups [Fig. 10H and I].

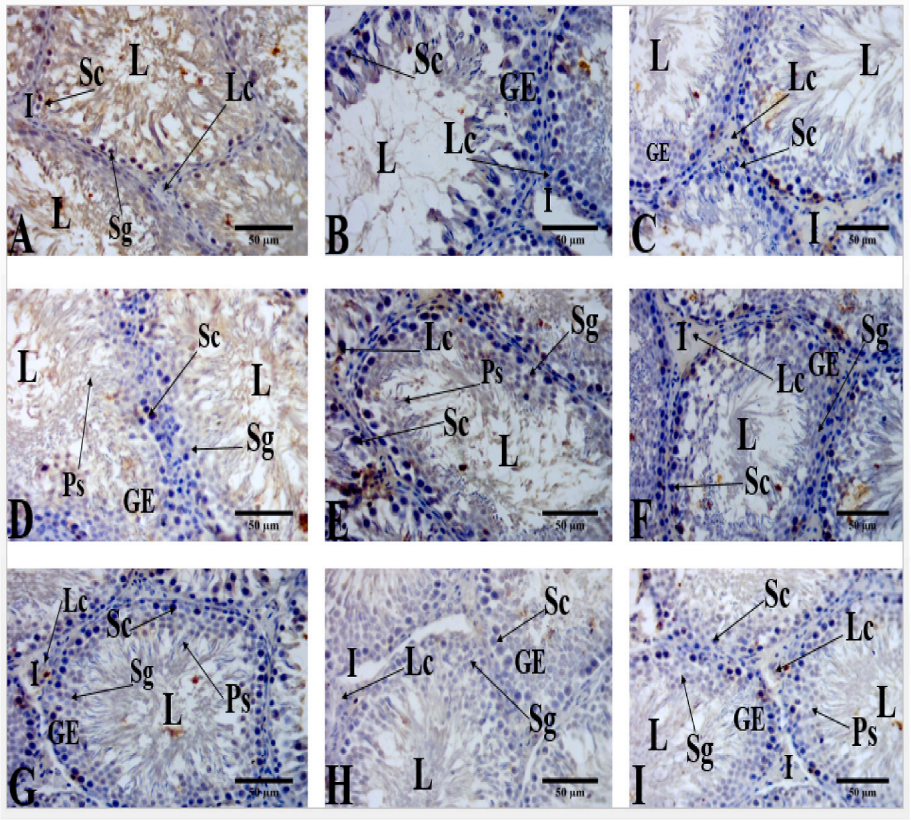

Fig. 8. Photomicrograph of testicular tissues of Immunohistochemical localization of BAX protein. Every type of germ cell demonstrates low to moderate BAX staining in the control group (A). Spermatogonia displayed strong staining, whereas spermatocytes and spermatids exhibited low to moderate BAX staining in the experimental group (B and G). The germ cells in the seminiferous tubules showed a weak BAX immunoreactivity Expression in groups (C, D, E, F, G, H, and I). In both the experimental groups and control groupA change in the location of BAX from the cytoplasm to the perinuclea can be observed in those selective germ cells. Several spermatogonia underwent BAX reorganization from cytoplasmic to nuclear localization. [Antibody-BAX, scale bar: 50 µm].
Abbreviations: Sg (spermatogonia); L (Lumen); I (interstitium); GE (germinal epithelium); LC (Leydig cells); Ps (primary spermatocyte).

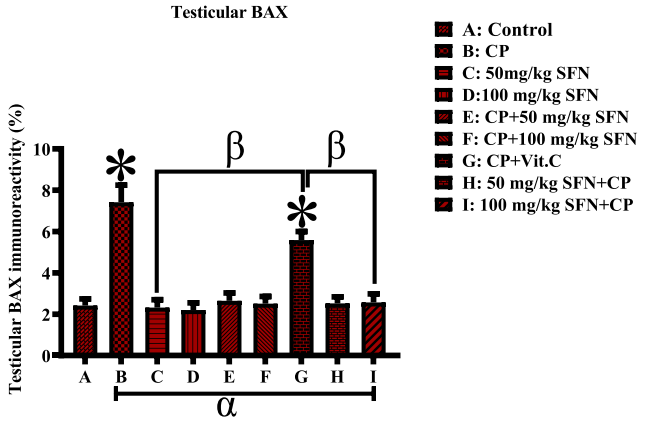

Fig. 9. Impacts of CP and 1-isothiocyanato-4-methylsulfonylbutane on testicular BAX immunoreactivity index of rats. Data expressed as Mean ± S.E.M, n = 10 in each group, *: represents a significant difference from control, α: represents a significant difference from CP, β: represents a significant difference from CP + Vit.C at ($p < 0.05$), One-Way ANOVA followed by Newman-Keuls multiple comparisons test.

3.11. Testicular BCL-2 immuno reactivity index

The testicular BCL-2 immunoreactivity index was significantly lower in the CP and CP + Vit.C treatment groups in contrast to the control group ($p < 0.05$). Meanwhile, SFN pre- and post-treatment groups showed a substantial increase in testicular BCL-2 immunoreactivity index in comparison to CP and CP + Vit.C therapy groups ($p < 0.05$). The testicular BCL-2 immunoreactivity index in the groups that received just SFN treatment rose insignificantly ($p > 0.05$) relative to the control group but significantly increased ($p < 0.05$) as compared to the CP alone exposure group. [Fig. 11].

4. Discussion

Apoptosis induction in germinal cells can be a factor in sperm count reduction (Adelakun et al., 2024b; Asadi et al., 2021). On the other hand, cisplatin (CP) disrupts intercellular connections and trigger induces apoptosis in Sertoli cells through the signaling pathway and triggers the mitochondrial pathway of apoptosis since these cells have a vital impact on spermatogenesis, which may be a reason for serious damage to the germinal cells (Köberle et al., 2024). According to previous studies and current observations, CP contributes to death in germinal, Sertoli, and Leydig cells by oxidative stress and apoptosis inducting (Lobo et al., 2020). Likewise, membrane lipid peroxidation induced by CP can fragment and disorganize spermatogenesis, Sertoli, and Leydig cells in the germinal epithelium, which causes them to be released into the lumen (Tharmalingam et al., 2020). This may be due to a decrease in the germinal epithelium thickness.

1-isothiocyanato-4-methyl sulfinylbutane (SFN) can cause the stability of membranes and prevent lipid peroxidation (Coutinho et al., 2023). Besides, SFN is a non-enzymatic defense system in testicular mitochondria (Ruhee and Suzuki, 2020). This supplement can inhibit

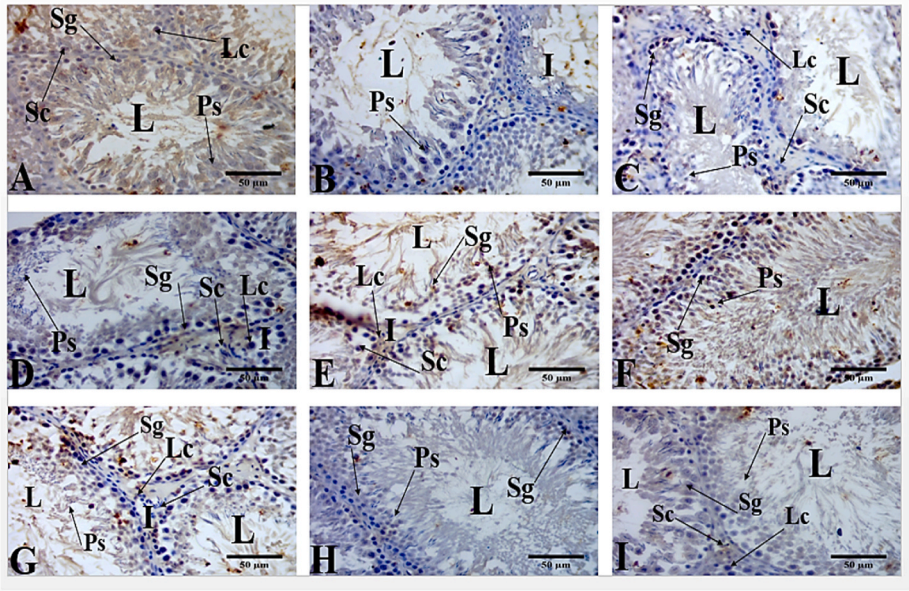

Fig. 10. Photomicrograph of testicular tissues of Immunohistochemical localization of BCL-2 protein. Observed moderate to intense BCL-2 staining in the control group (A). Decreased BCL-2 expression levels in the seminiferous tubules in group (B). Strong BCL-2 positivity was present in (C, D, E, F, G, H, and I). All varieties of germ cells in group (G) had high to moderate BCL-2 immunoreactivity labeling. BCL-2 was expressed in the cytoplasm and nuclei of spermatogonia, spermatocytes, and developing spermatids in both the control and experimental groups. BCL-2 was also selectively distributed at the luminal portion of mature spermatocytes and spermatids. [Antibody-BCL-2, scale bar: 50 µm].
Abbreviations: I (interstitium); LC (Leydig cells); GE (germinal epithelium); Sg (spermatogonia); L (Lumen); SC (Sertoli cells); Ps (primary spermatocyte).

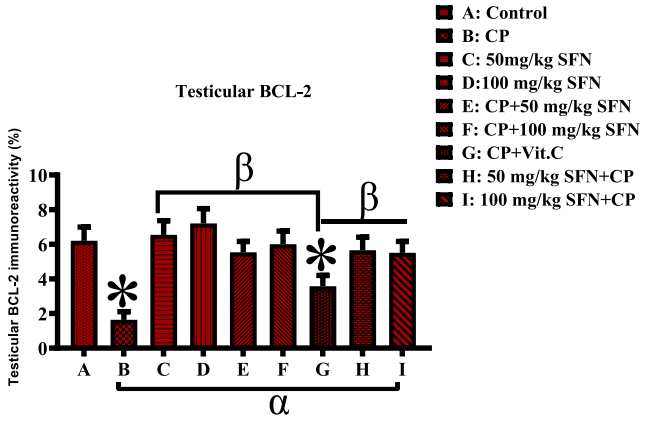

Fig. 11. Impacts of CP and 1-isothiocyanato-4-methyl sulfinylbutane on testicular BCL-2 immunoreactivity index of rats. Data expressed as Mean ± S.E. M, n = 10 in each group, *: represents a significant difference from control, α: represents a significant difference from CP, β: represents a significant difference from CP + Vit.C at ($p < 0.05$), One-Way ANOVA followed by Newman-Keuls multiple comparisons test.

oxidative damage in the testis and prevent apoptosis induction in spermatogenic, Sertoli, and Leydig cells (Yang et al., 2016). 1-isothiocyanato-4-methyl sulfinylbutane can return glutathione to its normal levels on the system's intracellular free radical scavenging and reduces oxidative stress levels (Mahn and Castillo, 2021). Treatment with SFN improves spermatogenesis in CP-treated rats by reducing peroxidation and oxidative stress, stabilizing cell membranes, and modulating testosterone levels.

Significant reductions in sperm chromatin condensation were seen in rats treated with CP along with oxidotoxicity in the testis and epididymal sperm, indicating a possible role for an altered redox state in this outcome. It is known that Glutathione (GSH) acts as an intermediate in sperm condensation and that the oxidation and reduction of sulfhydryl groups are essential to the sperm chromatin condensation/de-condensation process (Ulrich and Jakob, 2019). According to Tchounwou et al. (2021), there is a suggestion that CP might potentially impact Deoxyribonucleic acid (DNA) synthesis in germinal cells or obstruct the regular substitution of nuclear histones in germ cells for transition proteins and cysteine-rich protamines in spermatids during sperm chromatin condensation.

Semen samples taken from the epididymis of rats given CP treatment also showed a higher proportion of diploid germ cells. Targets of CP include tubulin and microtubules, which may disrupt chromosomal segregation and result in aneuploidy (Makovec, 2019). According to several research, CP can cause transforming and genotoxic effects such as aneuploidy and the creation of DNA adducts (Yimit et al., 2019; Meng et al., 2024). Exposure to cisplatin disrupted the course of meiotic DNA double-strand break repair and hampered chromosomal synapsis (Kiss et al., 2021). Accordingly, our evidence points to a connection between the development of aneuploidy and increased oxidative stress in germ cells as a result of CP exposure.

The sperm chromatin condensation process in this study was significantly protected by SFN, and the proportion of haploid cells rose. This suggests that appropriate sperm production requires a regulated redox state. According to Kaltsas (2023), sperm fertility is influenced by the interaction between the antioxidant defense system and SFN; thus, SFN may protect sperm chromatin throughout the process of sperm chromatin condensation and de-condensation.

Poor sperm DNA quality was identified as a major factor influencing male reproductive capabilities in both natural and aided conception (Kuchakulla et al., 2020). This verified previous findings that infertile men had a larger percentage of fragmented DNA spermatozoa than fertile men (Berte et al., 2021). Physical and environmental factors, illness, inflammation in male sexual organs, and sugar use have all been linked to sperm DNA fragmentation (Boublikova et al., 2024). The sperm's DNA integrity can be compromised by three mechanisms: faulty chromatin packing, apoptosis, and oxidative stress (Park et al., 2023). Reactive oxygen species (ROS) damage to male gametes is related to peroxidative reactions of sperm membrane components and DNA

breakage (Adelakun et al., 2019; Kutluyer et al., 2020). This might explain the rise in testicular MDA levels and DNA fragmentation seen in CP-exposed rats (Kitayama et al., 2022).

According to this study, the adverse consequences of CP go beyond reducing sperm quality and can damage sperm DNA by increased fragmentation. The three basic reasons for damage to sperm DNA are abnormal chromatin packing during spermiogenesis, abortive apoptosis, and excessive ROS production (Kuchakulla et al., 2020). Aitken's et al. (2020) argument is that peroxides interact with DNA bases, causing alterations and breakage. In contrast to the control group, CP injection increased the number of comets, and the percentage of DNA in the tail, tail lengths, and tail moment while lowering the percentage of DNA in the head and head length. Pretreatment and post-treatment with SFN, in contrast, resulted in a substantial reduction in CP-induced DNA damage and an increase in tail length in the treated. These protective and ameliorative advantages of SFN could be related it antioxidant capacity as a result, SFN reduces chromosomal aberrations in spermatozoa while increasing DNA synthesis.

This study found a link between SFN and spermatozoa's capacity to fertilize in rats. This could be because decreased peroxidation enhances the quality of sperm and reduces sperm DNA fragmentation, allowing sperm cells to penetrate the zona pellucida, or because the decrease in DNA fragmentation aids spermatozoons' ability to trigger the cascade of ooplasmic events that result in embryonic development and implantation capacity (Alahmar et al., 2022). The current study suggests that SFN reduces sperm DNA fragmentation caused by CP exposure and could be utilized as an ameliorative and preventative supplement for sperm in a patient undergoing CP treatment.

In this study, less cell proliferation was caused by cisplatin injury to the seminiferous tubules. Conversely, a significant increase in positive-TUNEL spermatogenesis cells and the degeneration of tight junctions between Sertoli cells in the CP group compared to the control group is indicated by a significant decrease in the population of spermatogenic, Sertoli, and Leydig cells, as well as by Tubule Differentiation Index (TDI), Spermatogenic Index (SPI), Sertoli Cell Index (SCI), and Meiosis Index (MI). These corroborate the findings of earlier research that exposure to varying dosages of CP resulted in a substantial decrease in sperm parameters, including count, viability, motility, and normal morphology (Köberle et al., 2024). As a result of damage to sperm membranes, proteins, and DNA brought on by increased oxidative stress, and reduction of sperm quality. This is manifested in alterations to the sperm membrane's fluidity, morphology, and peroxidation of unsaturated fatty acids in the plasma membrane (Ismail et al., 2023a,b). As a result, SFN pre-treatment and post-treatment improved CP-induced histopathological alteration in the testicular tissues, which may be connected to SFN's potent anti-inflammatory and antioxidant properties.

Furthermore, proapoptotic BAX and antiapoptotic BCL-2 are two important molecules implicated in cell death, and the BAX/BCL-2 ratio is the denominator that determines whether cells will undergo apoptosis (Spitz et al., 2021). The mitochondrial apoptotic pathway is controlled by proteins from the BCL-2 family, which controls cell survival and death (Czabotar and Garcia-Saez, 2023). In contrast, BAX protein, a pro-apoptotic factor, is elevated in oxidative stress conditions and impairs membrane permeability, leading to the cytosolic release of cytochrome C (Spitz and Gavathiotis, 2022). Cytosolic cytochrome C interacts with the apoptotic protease-activating factor to produce an apoptosome, which then promotes caspase-3, a critical factor in cell death (Flores-Romero et al., 2023). This results in DNA degradation, chromatin condensation, and the breakdown of bio-membrane proteins (Esteves et al., 2021). Cisplatin induces reproductive damage by activating mitochondrial apoptosis and raising the BAX/BCL-2 ratio (Seo et al., 2021). Apoptosis of the germinal epithelium has been identified as a probable mechanism for testicular injury after CP exposure. In the current study, SFN prevented apoptosis by decreasing BAX expression and increasing the expression of BCL-2 in the testis of CP-treated rats. The SFN's anti-apoptotic action may result from its anti-oxidative and anti-inflammatory properties.

The BCL-2 is found in the outer membrane of the mitochondria and supports cell survival by counteracting the effects of the proapoptotic protein BAX, hence maintaining mitochondrial membrane integrity (Morris et al., 2021). However, under oxidative stress, BAX enhances mitochondrial permeabilization, resulting in the discharge of both cytochrome C and ROS from the mitochondria into the cytoplasm (Yamazaki and Galluzzi, 2022). Cytochrome C interacts with the apoptotic protease activating factor 1 in the cytoplasm to produce an apoptosome, which then activates caspase-3, the essential regulator in the execution of apoptosis (Yamazaki and Galluzzi, 2022). This causes DNA fragmentation, chromatin condensation, and biomembrane protein degradation, as seen in the current work (Agarwal et al., 2020). In the current study, SFN pretreatment and intervention upregulate BCL-2 and downregulate BAX in the tissue of the testicles of CP-exposed rats this could be linked to the ant-apoptotic capabilities of SFN.

In comparison to controls, this study showed that the testes of rats injected with CP had significantly more apoptotic and necrotic cells. The anti-apoptotic protein BCL-2 expression levels in the same cells significantly decreased, which is consistent with these findings. There's a suggestion that germ cells underwent apoptosis as a reaction to oxidative stress caused by CP. According to Clay and Fox (2021), when DNA is broken, cells undergo cell cycle arrest to provide enough time for DNA repair processes to take effect and to initiate apoptotic mechanisms that lead to the elimination of damaged cells. The current results align with recent research that indicates a rise in BAX expression and a corresponding drop in BCL-2 expression levels, both at the protein and mRNA levels, after CP exposure (Cahyadi et al., 2022; Lopez et al., 2022).

The current results suggest that SFN has a high potential as a disease-modifying agent for the remedy of CP-induced testicular degeneration. As a result, the findings of this study provide an experimental foundation for the treatment of CP-induced testicular dysfunction using SFN. Furthermore, SFN pre-treatment and post-treatment are helpful for the prevention and amelioration of CP-induced testicular dysfunctions by stimulating germinal epithelial development and preserving the testicular cytoarchitecture from the detrimental effects of CP.

Furthermore, we, therefore, postulate that a single injection of cisplatin-induced testicular dysfunction. However, treatment with SFN in this study prevents and ameliorates the testicular damage caused by a single CP. As a result, SFN promotes spermatogenesis and reduces CP-induced oxidative stress via an antioxidant system of activities. Treatment with SFN effectively helps to protect and reverse testicular degeneration in this model and may be considered an adjunctive and emergency ameliorative agent in the treatment of testicular dysfunction induced by CP exposure and could be useful as prophylactic agents in cisplatin chemotherapy.

5. Conclusion

Cisplatin exposure induces histopathological alterations in testicular tissues by depleted germinal epithelium, widening and hypo-cellularity of the interstitium, sperm DNA fragmentation, and reduced sperm quality. However, the antapoptotic characteristics of SFN therefore, protect against cisplatin-induced apoptosis by controlling BCL-2 and BAX expression and ameliorating sperm DNA fragmentation.

CRediT authorship contribution statement

Sunday Aderemi Adelakun: Writing – original draft, Validation, Supervision, Project administration, Methodology, Investigation, Conceptualization. **Olalekan Wasiu Akintunde:** Writing – review & editing, Supervision, Methodology, Investigation, Conceptualization. **Babatunde Ogunlade:** Writing – original draft, Methodology, Investigation, Formal analysis, Conceptualization. **Akwu Bala Peter:** Writing – review & editing, Methodology, Investigation, Conceptualization. **Jacob**

Adewale Siyanbade: Writing – review & editing, Methodology, Investigation, Formal analysis, Conceptualization.

Conflicts of interest

As far as the publishing of this paper is concerned, the author affirms that there are no conflicts of interest.

Funding

This work was supported by Tartary Education Trust Fund (TETFUND) Intervention for Year 2021 Allocation for Academic Staff Training and Development (AST&D) grant no. FUTA/VCPU/TETFund/155 awarded to Sunday Aderemi Adelakun.

Declaration of competing interest

The authors declare that they have no known competing financial interests or personal relationships that could have appeared to influence the work reported in this paper.

Authors declare that they have no known competing interests.

Abbreviations

ANOVA	Analysis of Variance
CP	Cisplatin
DNA	Deoxyribonucleic acid
ELISA	Enzyme-Linked Immunosorbent Assay
GSH	Glutathione
GE	Germinal epithelium
I	Interstitium
LC	Leydig cells
L	Lumen
PBS	Phosphate buffered saline
ROS	Reactive oxygen species
RNS	Reactive Nitrogen Species
MDA	Malondialdehyde
Sg	Spermatogonia
Sg	Spermatogonia
SFN	1-isothiocyanato-4-methyl sulfinylbutane
SDF	Sperm DNA fragmentation

References

Adelakun, S.A., Ogunlade, B., Aniah, J.A., Akwu, B.P., Afolabi, M.O., 2024a. Excessive Caffeine Intake inhibits steroidogenesis, and folliculogenesis and disrupts utero-ovarian tissue histomorphology integrity in experimental rats, and precipitates polycystic ovary syndrome in Sprague-Dawley rats. Food Chemistry Advance, 100678.

Adelakun, S.A., Akintunde, O.W., Jeje, S.O., Alao, O.A., 2022b. Ameliorating and protective potential of 1-isothiocyanates-4-methyl sulfonyl butane on cisplatin-induced oligozoospermia and testicular dysfunction via redox-inflammatory. Phytomedicine, 100268.

Adelakun, S.A., Akingbade, G.T., Aniah, J.A., Modupeoluwa, O.O., 2017. Histomorphological and biochemical assessment of testicular parameters following oral administration of cadmium nitrate to adult male wistar rats. European Journal of Biomedical 4 (6), 36–43.

Adelakun, S.A., Akintunde, O.W., Akingbade, G.T., Adedotun, O.A., 2022a. Bioactive component of aqueous extract of Solanum melongena ameliorate estradiol valerate induced ovarian-pituitary dysfunctions in female Sprague–Dawley rats: histomorphological and biochemical evidence. Phytomedicine 2, 100175.

Adelakun, S.A., Akintunde, O.W., Ogunlade, B., Adeyeluwa, B.E., 2023a. Histochemical and histomorphological evidence of the modulating role of 1-isothiocyanate-4-methyl sulfonyl butane on cisplatin-induced testicular-pituitary axis degeneration. Morphologie 107 (356), 80–98.

Adelakun, S.A., Aniah, J.A., Omotoso, O.D., Arowosegbe, O.A., 2024b. Anti-hepatopathy and anti-nephropathy activities of Taraxacum officinale in a rat model of Streptozotocin diabetes-induced hepatorenal toxicity and dyslipidemia via attenuation of oxidative stress, inflammation, apoptosis, electrolyte imbalances, and mitochondrial dysfunction. Aspects of Molecular Medicine 3, 100034.

Adelakun, S.A., Ogunlade, B., Iteire, K.A., Adedotun, O.A., 2021a. Ameliorating potential and fertility-enhancing activities of nutritional dietary supplementation of D-Ribose -l-Cysteine in cisplatin-induced oligoasthenoteratozoospermia and seminiferous epithelium degeneration in adult male Sprague-Dawley rats. Metabol Open 12, 100128.

Adelakun, S.A., Ogunlade, B., Siyanbade, J.A., Chukwunenye, C.C., 2023b. Evaluation of the ameliorative potential of Nutritional Dietary supplementation of vitamin B_{12} following chronic tramadol hydrochloride exposure induced hyperlipidemia, atherogenic indices, and hepato-renal dysfunction by downregulating redox imbalance, NO/iNOS/NF-κB response, caspase-3- activation and DNA fragmentation in rat's model. Food Chemistry Advances 2, 100286.

Adelakun, S.A., Ukwenya, V.O., Ogunlade, B.S., Aniah, J.A., Ibiayo, A.G., 2019. Nitrite-induced testicular toxicity in rats: therapeutic potential of walnut oil. JBRA Assisted Reproduction 23 (1), 15–23, 2019.

Adelakun, S.A., Ukwenya, V.O., Akintunde, O.W., 2021c. Vitamin B_{12} ameliorates Tramadol-induced oxidative stress, endocrine imbalance, apoptosis, and NO/iNOS/NF-κB expression in Sprague Dawley through the regulatory mechanism in the pituitary-gonadal axis. Tissue Cell, 101697.

Adelakun, S.A., Ukwenya, V.O., Akingbade, G.T., Omotoso, O.D., Aniah, J.A., 2020. Interventions of aqueous extract of Solanum melongena fruits (garden eggs) on mercury chloride-induced testicular toxicity in adult male Wistar rats. Biomed. J. 43 (2), 174–182.

Adelakun, S.A., Akinola, B.K., Akingbade, G.T., 2018. Fertility enhancing activities of bioactive components of *Cochlospermum splanchnic rhizome*on cisplatin induced reproductive dysfunctions in Sprague- dawley rats. J. Fam. Reprod. Health 12 (3), 148–159, 2018.

Adelakun, S.A., Ogunlade, B., Olawuyi, T.S., Ojewale, A.O., 2021b. Aqueous extract of *Tetrapleura tetraptera* fruit peels influence copulatory behavior and maintain testicular integrity in sexually mature male Sprague-Dawley rats: pro-fertility evaluation and histomorphometry evidence. Current research in physiology 4, 7–16.

Agarwal, A., Majzoub, A., Baskaran, S., Panner, S.M.K., Cho, C.L., Henkel, R., et al., 2020. Sperm DNA fragmentation: a new guideline for clinicians. World J Mens Health 38 (4), 412–471.

Agbaje, I.M., Rogers, D.A., McVicar, C.M., McClure, N., Atkinson, A.B., Mallidis, C., et al., 2007. Insulin dependant diabetes mellitus: implications for male reproductive function. Hum. Reprod. 22, 1871–1877.

Aitken, R.J., Whiting, S., Connaughton, H., Curry, B., Reinheimer, T., van Duin, M.A., 2020. Novel pathway for the induction of DNA damage in human spermatozoa involving extracellular cell-free DNA. Mutat. Res. 821, 111722.

Alahmar, A.T., Singh, R., Palani, A., 2022. Sperm DNA fragmentation in reproductive medicine: a review. J. Hum. Reprod. Sci. 15 (3), 206–218.

Asadi, A., Ghahremani, R., Abdolmaleki, A., Rajaei, F., 2021. Role of sperm apoptosis and oxidative stress in male infertility: a narrative review. Int J Reprod Biomed. 19 (6), 493–504.

Atalay, U.B., Ilhan, F., Gulyuz, F., 2012. The effects of sildenafil citrate and vitamins A. C and E on testicular damage in alloxan-diabetic rats. J. Anim. Vet. Adv. 11, 56–63.

Aydogan, M., Barlas, N., 2006. Effects of maternal 4-tert octylphenol exposure on the reproductive tract of male rats at adulthood. Reprod. Toxicol. 22, 455–460.

Berte, N., Eich, M., Heylmann, D., Koks, C., Van Gool, S.W., Kaina, B., 2021. Impaired DNA repair in mouse monocytes compared to macrophages and precursors. DNA Repair 98, 103037.

Bhardwaj, J.K., Panchal, H., 2021. Quercetin mediated attenuation of cadmium-induced oxidative toxicity and apoptosis of spermatogenic cells in caprine testes in vitro. Environ. Mol. Mutagen. 62 (6), 374–384.

Boublikova, L., Matouskova, L., Bakardjieva-Mihaylova, V., Zwyrtkova, M., Skvarova-Kramarzova, K., et al., 2024. Novel molecular aberrations involved in testicular germ cell tumor (TGCT) development and cisplatin resistance, 42 (4), 520.

Bozic, D., Baralić, K., Živančević, K., Miljaković, E.A., Ćurčić, M., Antonijević, B., et al., 2022. Predicting sulforaphane-induced adverse effects in colon cancer patients via in silico investigation. Biomed. Pharmacother. 146, 112598.

Cahyadi, A., Ugrasena, I.D.G., Andarsini, M.R., Larasati, M.C.S., Aryati, A., Arumsari, D. K., 2022. Relationship between bax and bcl-2 protein expression and outcome of induction phase chemotherapy in pediatric acute lymphoblastic leukemia. Asian Pac J Cancer Prev 23 (5), 1679–1685.

Clay, D.E., Fox, D.T., 2021. DNA damage responses during the cell cycle: insights from model organisms and beyond. Genes 12 (12), 1882.

Coscueta, E.R., Sousa, A.S., Reis, C.A., Pintado, M.M., 2022. Phenylethyl isothiocyanate: a bioactive agent for gastrointestinal health. Molecules 27, 794.

Coutinho, L.L., Junior, T.C.T., Rangel, M.C., 2023. Sulforaphane: an emergent anti-cancer stem cell agent. Front. Oncol. 13, 1089115.

Czabotar, P.E., Garcia-Saez, A.J., 2023. Mechanisms of BCL-2 family proteins in mitochondrial apoptosis. Nat. Rev. Mol. Cell Biol. 24, 732–748.

Dey, P., Mondal, A.K., Singh, S.K.S.K., Singh, M.Ch M.S., Harpreet, V., 2000. Quantitation of spermatogenesis by DNA flow cytometry from fine needle aspiration cytology material. Diagn. Cytopathol. 23, 386–387.

Donnelly, E.T., McClure, N., Lewis, S.E., 1999. The effect of ascorbate and alpha-tocopherol supplementation in vitro on DNA integrity and hydrogen peroxide-induced DNA damage in human spermatozoa. Mutagenesis 14, 505–512.

Elham, G., Vahid, N., Mozafar, K., 2016. Antioxidant and protective effects of Royal jelly on histopathological changes in the testis of diabetic rats. Int J Reprod Biomed 14 (8), 519–526.

Esteves, S.C., Zini, A., Coward, R.M., Evenson, D.P., Gosálvez, J., Lewis, S.E.M., Sharma, R., Humaidan, P., 2021. Sperm DNA fragmentation testing: summary evidence and clinical practice recommendations. Andrologia 53 (2), e13874.

Flores-Romero, H., Dadsena, S., García-Sáez, A.J., 2023. Mitochondrial pores at the crossroad between cell death and inflammatory signaling. Mol. Cell. 83, 843–856.

Hacker-Klom, U.B., Göhde, W., Nieschlag, E., Behre, H.M., 1999. DNA flow cytometry of human semen. Hum. Reprod. 14, 2506–2512.

Hamed, I.A., Sherif, R.M., El-Sheikh, E.A., Aldawek, A.M., Shalaby, A.A., 2023. Protective effect of vitamin C against thiamethoxam-induced toxicity in male rats. Open Vet. J. 13 (10), 1334–1345.
Hong, B., Chapa, V., Saini, U., Modgil, P., Cohn, D.E., He, G., et al., 2021. Oncolytic HSV therapy modulates vesicular trafficking inducing cisplatin sensitivity and antitumor immunity. Clin. Cancer Res. 27 (2), 542–553.
Hughes, C.M., Lewis, S.E., McKelvey, M.V.J., Thompson, W., 1997. Reproducibility of human sperm DNA measurements using the alkaline single-cell gel electrophoresis assay. Mutat. Res. 374, 261–268.
Ismail, H.Y., Shaker, N.A., Hussein, S., Tohamy, A., Fathi, M., Rizk, H., Wally, Y.R., 2023a. Cisplatin-induced azoospermia and testicular damage ameliorated by adipose-derived mesenchymal stem cells. Biol. Res. 56 (1), 2.
Ismail, H.Y., Shaker, N.A., Hussein, S., Tohamy, A., Fathi, M., Rizk, H., Wally, Y.R., 2023b. Cisplatin-induced azoospermia and testicular damage ameliorated by adipose-derived mesenchymal stem cells. Biol. Res. 56 (1), 2, 19.
Juan, W.S., Lin, H.W., Chen, Y.H., Chen, H.Y., Hung, Y.C., Tai, S.H., et al., 2012. Optimal percoll concentration facilitates flow cytometric analysis for annexin V/propidium iodine-stained ischemic brain tis sues. Cytometry 81, 400–408.
Kaiser, A.E., Baniasadi, M., Giansiracusa, D., Giansiracusa, M., Garcia, M., Fryda, Z., Wong, T.L., Bishayee, A., 2021. Sulforaphane: a broccoli bioactive phytocompound with cancer preventive potential. Cancers 13, 4796.
Kalpana, D.D., Gayathri, R., Gunassekaran, G.R., Murugan, S., Sakthisekaran, D., 2013. Apoptotic role of natural isothiocyanate from broccoli (Brassica oleracea italica) in experimental chemical lung carcinogenesis. Pharm. Biol. 51 (5), 621–628.
Kaltsas, A., 2023. Oxidative stress and male infertility: the protective role of antioxidants. Medicina (Kaunas) 59 (10), 1769.
Kamal, M.M., Akter, S., Lin, C.N., Nazzal, S., 2020. Sulforaphane as an anticancer molecule: mechanisms of action, synergistic effects, enhancement of drug safety, and delivery systems. Arch Pharm. Res. (Seoul) 43, 371–384.
Kamal, R.M., Abdull-Razis, A.F., Mohd-Sukri, N.S., Perimal, E.K., Ahmad, H., Patrick, R., et al., 2022. Beneficial health effects of glucosinolates-derived isothiocyanates on cardiovascular and neurodegenerative diseases. Molecules 27, 624.
Kiss, R.C., Xia, F., Acklin, S., 2021. Targeting DNA damage response and repair to enhance therapeutic index in cisplatin-based cancer treatment. Int. J. Mol. Sci. 22 (15), 8199.
Kitayama, S., Ikeda, K., Sato, W., Takeshita, H., Kawakami, S., Inoue, S., Horie, K., 2022. Testis-expressed gene 11 inhibits cisplatin-induced DNA damage and contributes to chemoresistance in testicular germ cell tumor. Sci. Rep. 12, 18423.
Köberle, B., Usanova, S., Piee-Staffa, A., Heinicke, U., Clauss, P., Brozovic, A., Kaina, B., 2024. Strong apoptotic response of testis tumor cells following cisplatin treatment. Int. Urol. Nephrol. 56 (3), 1007–1017.
Kuchakulla, M., Narasimman, M., Khodamoradi, K., Khosravizadeh, Z., Ramasamy, R., 2020. How defective spermatogenesis affects sperm DNA integrity. Andrologia 53, 13615.
Kutluyer, F., Çakir, S.Y., Kocabaş, M., Aksu, Ö., 2020. Sperm quality and oxidative stress in chub Squalius orientalis and Padanian barbel Barbus plebejus (Teleostei: cyprinidae) after in vitro exposure to low doses of bisphenol A. Drug Chem. Toxicol. 7, 1–6.
Li, H., Spade, D.J., 2021. Reproductive Toxicology: environmental exposures, fetal testis development, and function: phthalates and beyond. Reproduction 162 (5), F147–F167.
Liu, S.W., Li, H.T., Ge, R.S., Cheng, C.Y., 2021. NC1-peptide derived from collagen α3 (IV) chain is a blood-tissue barrier regulator: a lesson from the testis. Asian J. Androl. 23 (2), 123–128.
Lobo, J., Jerónimo, C., Henrique, R., 2020. Cisplatin resistance in testicular germ cell tumors: current challenges from various perspectives. Cancers 12 (6), 1601.
Lopez, A., Reyna, D.E., Gitego, N., Felix, K., Hua, Z., Miguel, A.M., et al., 2022. Co-targeting of BAX and BCL-XL proteins broadly overcomes resistance to apoptosis in cancer. Nat. Commun. 13, 1199.
Mahn, A., Castillo, A., 2021. Potential of sulforaphane as a natural immune system enhancer: a review. Molecules 26 (3), 752.
Mahn, A., Pérez, C.E., Zambrano, V., Barrientos, H., 2022. Maximization of sulforaphane content in broccoli sprouts by blanching. Foods 11, 1906.
Makled, M.N., Said, E., 2021. Tranilast abrogates cisplatin-induced testicular and epididymal injuries: an insight into its modulatory impact on apoptosis/proliferation. J. Biochem. Mol. Toxicol. 35 (8), e22817.
Makovec, T., 2019. Cisplatin and beyond molecular mechanisms of action and drug resistance development in cancer chemotherapy. Radiol. Oncol. 53 (2), 148–158.
Malmir, M., Soleimani, M.M., Naderi, N.S., Faraji, T., 2018. Protective antioxidant effects of N-acetylcysteine against impairment of spermatogenesis caused by paranonylphenol. Andrologia 50 (10), e13114.
Mangla, B., Javed, S., Sultan, M.H., Kumar, P., Kohli, K., Najmi, A., et al., 2021. Sulforaphane: a review of its therapeutic potentials, advances in its nano delivery, recent patents, and clinical trials. Phytother Res. 35 (10), 5440–5458.
Mehranjani, M.S., Taefi, R., 2012. The protective role of vitamin E on the testicular tissue in rats exposed to sodium arsenite during the prenatal stage till sex maturity: a stereological analysis. Iran J Reprod Med 10 (6), 571.
Meng, X., Ma, F., Yu, D., 2024. The diverse effects of cisplatin on tumor microenvironment: insights and challenges for the delivery of cisplatin by nanoparticles. Environ. Res. 240 (1), 117362.
Moreira, M.V., Pereira, S.C., Guerra-Carvalho, B., Carrageta, D.F., Pinto, S., Barros, A., et al., 2022. Hyperoside supplementation in preservation media surpasses vitamin C protection against oxidative stress-induced damage in human spermatozoa. Cell. Physiol. Biochem. 56 (1), 1–23.
Morris, J.L., Gillet, G., Prudent, J., Popgeorgiev, N., 2021. Bcl-2 family of proteins in the control of mitochondrial calcium signalling: an old chap with new roles. Int. J. Mol. Sci. 22 (7), 3730.
Nandini, D.B., Rao, R.S., Deepak, B.S., Reddy, P.B., 2020. Sulforaphane in broccoli: the green chemoprevention!! Role in cancer prevention and therapy. J. Oral Maxillofac. Pathol. 24, 405.
National Institute of Health (NIH), 1985. Guide for the Care and the Use of Laboratory Animals, vol. 20. National Institute of Health, Bethesda, pp. 85–123.
Oderinde, O., Noronha, C., Oremosu, A., Kusemiju, T., Okonlawon, A., 2002. Abortifacient properties of aqueous extract of Carica papaya (Linn) seed on female Sprague–Dawley rats. Niger. Postgrad. Med. J. 9, 95, 8.
Ogunlade, B., Adelakun, S.A., Iteire, K., 2020. Sulforaphane response on aluminum-induced oxidative stress, alterations in sperm characterization and testicular histomorphometry in Wistar rats. International Journal of Reproductive BioMedicine 18, 611–624.
Ogunlade, B., Adelakun, S.A., Ukwenya, V.O., Elemoso, T.T., 2021. Potentiating response of D- Ribose-L-Cysteine on Sodium arsenate-induced hormonal imbalance, spermatogenesis impairments and histomorphometric alterations in adult male Wistar rat. JBRA Assist Reprod 25 (3), 358–367.
Olawuyi, T.S., Akinola, B.K., Adelakun, S.A., Ogunlade, B.S., Akingbade, G.T., 2019. Effects of aqueous leaf extract of *Lawsonia inermis* on aluminum induced oxidative stress and adult wistar rat pituitary gland histology. JBRA Assisted Reproduction 23 (2), 117–122, 2019.
Olayanju, J.B., Bozic, D., Naidoo, U., Sadik, O.A., 2024. A comparative review of key isothiocyanates and their health benefits. Nutrients 16 (6), 757.
Park, J., Luo, Y., Park, J.W., Kim, S.H., Hong, Y.J., Lim, Y., Seo, Y., Bae, J., Seo, S.B., 2023. Downregulation of DNA methylation enhances differentiation of THP-1 cells and induces M1 polarization of differentiated macrophages. Sci. Rep. 13, 13132.
Rafiei, H., Ashrafizadeh, M., Ahmadi, Z., 2020. MicroRNAs as novel targets of sulforaphane in cancer therapy: the beginning of a new tale? Phytother Res. 34, 721–728.
Rahimi, A., Asadi, F., Rezghi, M., Kazemi, S., Soorani, F., Memariani, Z., 2022. Natural products against cisplatin-induced male reproductive toxicity: a comprehensive review. J. Biochem. Mol. Toxicol. 36 (3), e22970.
Ranasinghe, R., Mathai, M.L., Zulli, A., 2022. Cisplatin for cancer therapy and overcoming chemoresistance. Heliyon 8 (9), e10608.
Ratnasooriya, W.D., Dharmasiri, M.G., 2000. Effects of Terminalia catappa seeds on sexual behaviour and fertility of male rats. Asian J. Androl. 2, 213–219.
Rezvanfar, M., Sadrkhanlou, R., Ahmadi, A., Shojaei-Sadee, H., Rezvanfar, M., Mohammadirad, A., Salehnia, A., Abdollahi, M., 2008. Protection of cyclophosphamide-induced toxicity in reproductive tract histology, sperm characteristics, and DNA damage by an herbal source; evidence for role of free-radical toxic stress. Hum. Exp. Toxicol. 27 (12), 901–910.
Ruhee, R.T., Suzuki, K., 2020. The integrative role of sulforaphane in preventing inflammation, oxidative stress and fatigue: a review of a potential protective phytochemical. Antioxidants 9 (6), 521.
Sasso-Cerri, E., 2009. Enhanced ERbeta immunoexpression and apoptosis in the germ cells of cimetidine-treated rats. Reprod. Biol. Endocrinol. 7, 127.
Sayyed, A.A., Gondaliya, P., Mali, M., Pawar, A., Bhat, P., Khairnar, A., et al., 2021. MiR-155 inhibitor-laden exosomes reverse resistance to cisplatin in a 3D tumor spheroid and xenograft model of oral cancer. Mol. Pharm. 18 (8), 3010–3025.
Selvaraju, V., Baskaran, S., Agarwal, A., Henkel, R., 2021. Environmental contaminants and male infertility: effects and mechanisms. Andrologia 53 (1), e13646.
Seo, D.Y., Bae, J.H., Zhang, D., Song, W., Kwak, H.B., Heo, J.W., et al., 2021. Effects of cisplatin on mitochondrial function and autophagy-related proteins in skeletal muscle of rats. BMB Rep 54 (11), 575–580.
Spitz, A.Z., Gavathiotis, E., 2022. Physiological and pharmacological modulation of BAX. Trends Pharmacol. Sci. 43, 206–220.
Spitz, A.Z., Zacharioudakis, E., Reyna, D.E., Garner, T.P., Gavathiotis, E., 2021. Eltrombopag directly inhibits BAX and prevents cell death. Nat. Commun. 12, 1134.
Tchounwou, P.B., Dasari, S., Noubissi, F.K., Ray, P., Kumar, S., 2021. Advances in our understanding of the molecular mechanisms of action of cisplatin in cancer therapy. J. Exp. Pharmacol. 13, 303–328.
Tharmalingam, M.D., Matilionyte, G., Wallace, W.H.B., Stukenborg, J.B., Jahnukainen, K., Oliver, E., et al., 2020. Cisplatin and carboplatin result in similar gonadotoxicity in immature human testis with implications for fertility preservation in childhood cancer. BMC Med. 18 (1), 374.
Tuominen, V.J., Ruotoistenmäki, S., Viitanen, A., Jumppanen, M., Isola, J., 2010. ImmunoRatio: a publicly available web application for quantitative image analysis of estrogen receptor (ER), progesterone receptor (PR), and Ki-67. Breast Cancer Res. 12 (4), R56.
Ucheya, R.E., Biose, I.J., 2010. Teratogenic effects of methanolic extract of Ricinus communis seed oil on the morphology of fetal Wistar rats. Biosci Biotechnol Res Asia. 7, 719–723.
Ukwenya, V.O., Olawuyi, T.S., Adelakun, S.A., Ogunsola, O.I., Ukwenya, M.U., 2020. D-ribose-L-cysteine improves hormonal imbalance, spermatogenic dysregulation, and redox status in streptozotocin-diabetic rats. Comp. Clin. Pathol. 29 (6), 1107–1117.
Ulrich, K., Jakob, U., 2019. The role of thiols in antioxidant systems. Free Radic. Biol. Med. 140, 14–27.
Vindelov, L.L., 1977. Flow microfluorometric analysis of nuclear DNA in cells from solid tumors and cell suspensions. A new method for rapid isolation and straining of nuclei. Virchows Arch. B Cell Pathol. 24, 227–242.
Wu, J., Shi, Y., Zhou, M., Chen, M., Ji, S., et al., 2024. Nutrient vitamins enabled metabolic regulation of ferroptosis via reactive oxygen species biology. Front. Pharmacol. 15, 1434088.

Yadegari, M., Zare, M.F., Rezvani, M.E., Dortaj, H., Pourentezari, Z.M., 2024. Effect of vitamin C on histomorphometric changes of testis, epididymis, prostate, and seminal vesicle induced by acrylamide in rat. Naunyn-Schmiedeberg's Arch. Pharmacol. 397 (1), 549–557.
Yamazaki, T., Galluzzi, L., 2022. BAX and BAK dynamics control mitochondrial DNA release during apoptosis. Cell Death Differ. 29, 1296–1298.
Yan, Q., Li, T., Zhang, Y., Zhao, X., Wang, Q., Yuan, L., 2024. Caveolin 1 regulates the tight junctions between Sertoli cells and promotes the integrity of blood-testis barrier in yak via the FAK/ERK signaling pathway. Animals (Basel) 14 (2), 183.
Yang, S.H., Long, M., Yu, L.H., Li, L., Li, P., Zhang, Y., et al., 2016. Sulforaphane prevents testicular damage in kunming mice exposed to cadmium via activation of Nrf2/ARE signaling pathways. Int. J. Mol. Sci. 17 (10), 1703.
Yimit, A., Adebali, O., Sancar, A., Jiang, Y., 2019. Differential damage and repair of DNA adducts induced by anti-cancer drug cisplatin across mouse organs. Nat. Commun. 10, 309.
Zylinska, L., Lisek, M., Guo, F., Boczek, T., 2023. Vitamin C modes of action in calcium-involved signaling in the brain. Antioxidants 12, 231.